Determination of e/h, Using Macroscopic Quantum Phase Coherence in Superconductors. I. Experiment*

W. H. PARKER,† D. N. LANGENBERG, AND A. DENENSTEIN‡
Department of Physics and Laboratory for Research on the Structure of Matter, University of Pennsylvania, Philadelphia, Pennsylvania 19104

AND

B. N. TAYLOR
RCA Laboratories, Princeton, New Jersey 08540

(Received 15 July 1968)

The fundamental physical constant e/h has been experimentally determined with high accuracy, using the ac Josephson effect in systems of weakly coupled superconductors (Josephson junctions). The measurement depends on the validity of the Josephson frequency-voltage relation $\nu=2eV/h$, which relates the frequency of the oscillating supercurrent between two weakly coupled superconductors to the potential difference between them. The frequency-voltage ratio was measured using two effects: (a) constant-voltage steps induced in the dc current-voltage characteristics of Josephson junctions by microwave radiation and (b) microwave radiation emission by Josephson junctions biased at nonzero voltages. The ratio was found to be independent of the type of superconductor and the type of Josephson junction used, nonlinear harmonic and subharmonic effects, temperature, magnetic field, and microwave power and frequency. These results justify confidence in the general validity of the Josephson frequency-voltage relation and in the identification of the frequency-voltage ratio with $2e/h$. The final experimental result is $2e/h=483.5976\pm0.0012$ MHz/μV_{NBS} (standard deviation) referred to the volt as maintained by the U. S. National Bureau of Standards prior to January 1, 1969. The result in terms of the NBS volt as maintained after this date, V_{69NBS}, is 483.5935 ± 0.0012 MHZ/μ_{69NBS}.

I. INTRODUCTION

THE central concept in our current understanding of the phenomenon of superconductivity is that the superconducting state is a highly correlated phase-coherent quantum state of macroscopic scale. This idea was proposed by London[1] as early as 1935 and is an essential feature of the phenomenological theory of superconductivity of Ginsburg and Landau[2] and the microscopic theory of Bardeen, Cooper, and Schrieffer[3] (BCS). London pointed out that the existence of such a phase-coherent state, together with requirements of gauge invariance which relate the phase to the magnetic vector potential, implies that the magnetic flux linking a multiply connected superconductor must be quantized in units of hc/Q, where Q is the charge of the fundamental current carrying entity in the superconducting state. This prediction was strikingly confirmed by the experimental observation of flux quantization in 1961 by Deaver and Fairbank[4] and by Doll and Näbauer.[5] These experiments further indicated that, to an accuracy of a few percent, Q is equal to twice the electronic charge, in accordance with the BCS theory in which bound electron pairs play a central role.

In 1962 Josephson announced several remarkable theoretical predictions relating to the behavior of systems in which the phase-coherent states of two superconductors are weakly coupled.[6] The original theory was applied to the case of two superconductors separated by an insulating barrier, where the coupling is due to the tunneling of bound electron pairs through the barrier from one superconductor to the other. It has since become clear that the necessary weak coupling can be achieved in other ways and that the phenomena predicted by Josephson occur quite generally in a variety of systems. Experimental and theoretical investigations of these Josephson effects have proceeded at a rapid pace. They have become established as extremely powerful tools for the study of phase coherence in superconductors and as the basis for devices with unique and far-reaching capabilities.[7] We are here

* Supported by the National Science Foundation and the Advanced Research Projects Agency. This paper is based on a thesis submitted by W. H. Parker in partial fulfillment of the requirements for the Ph.D. degree at the University of Pennsylvania.

† Present address: Physics Department, University of California, Irvine, Calif.

‡ Present address: National Bureau of Standards, Gaithersburg, Md.

[1] F. London, Proc. Roy. Soc. (London) **A152**, 24 (1935); Phys. Rev. **74**, 562 (1948); *Superfluids* (John Wiley & Sons, Inc., New York, 1950).

[2] V. L. Ginsburg and L. D. Landau, Zh. Eksperim. i Teor. Fiz. **20**, 1064 (1950).

[3] J. Bardeen, L. N. Cooper, and J. R. Schrieffer, Phys. Rev. **106**, 162 (1957); **108**, 1175 (1957).

[4] B. S. Deaver, Jr., and William M. Fairbank, Phys. Rev. Letters **7**, 43 (1961); see also A. L. Kwiram and B. S. Deaver, Jr., *ibid.* **13**, 189 (1964).

[5] R. Doll and M. Näbauer, Phys. Rev. Letters **7**, 51 (1961).

[6] B. D. Josephson, Phys. Letters **1**, 251 (1962).

[7] For recent reviews of the experimental and theoretical situation, see the lectures by D. J. Scalapino, J. E. Mercereau, D. N. Langenberg, and A. F. G. Wyatt [in *Tunneling Phenomena in Solids*, edited by E. Burstein and S. Lundquist (Plenum Press, Inc., New York, 1969)], the review article by P. W. Anderson [in *Progress in Low Temperature Physics*, edited by C. J. Gorter (North-Holland Publishing Co., Amsterdam, 1967), Vol. 5], and the article by J. E. Mercereau [in *Superconductivity*, edited by R. D. Parks (M. Dekker, New York, 1969)]. Devices based on the Josephson effects have been reviewed by B. N. Taylor, J. Appl. Phys. **39**, 2490 (1968).

particularly concerned with the ac Josephson effect. Beginning with quite general assumptions about the nature of the phase-coherent superconducting state, it can be shown theoretically that if a pair of weakly coupled superconductors (a Josephson junction) are maintained at a relative dc potential V, an alternating supercurrent with frequency

$$\nu = 2eV/h \tag{1}$$

flows between the superconductors. A host of different experiments have left no doubt as to the existence of this ac supercurrent and have elucidated its properties in considerable detail.[7] Its most notable property is expressed by the Josephson frequency-voltage relation (1). It is believed on theoretical grounds that this relation is a general and exact characteristic of the ac supercurrent between weakly coupled bulk superconductors, independent of the detailed properties of the materials, geometry, or environment of the system. This purported generality and the central role played by the frequency-voltage relation invite rigorous experimental testing. The relation involves just two experimental variables: a frequency and a dc voltage. The accuracy with which these quantities can be measured makes possible a quantitative experimental test of the frequency-voltage relation with an accuracy several orders of magnitude beyond the level that has been achieved in the measurement of other fundamental parameters associated with the superconducting state, e.g., the flux quantum. We have undertaken to make such a test, and this paper is in part a report of the results.

The work reported here was also motivated by another consideration. If Eq. (1) is assumed to be correct and exact (including the factor 2), then obviously a measurement of the frequency-voltage ratio determines the fundamental physical constant e/h. When one contemplates this possibility, three questions arise: First, can the frequency-voltage ratio be measured sufficiently accurately to yield a value of e/h competitive with values obtained by other methods? Second, can the frequency-voltage ratio really be identified with $2e/h$? Third, is a new determination of e/h sufficiently important to warrant the special effort required in any experiment which purports to determine a fundamental constant? The justifications for an affirmative answer to the third question are related to the details of the experimental basis for our present knowledge of the fundamental constants and will be discussed at length in a future paper (hereafter referred to as II).[8] The present paper is concerned with the first two questions. The answer to the first question depends on establishing experimentally that there are no aspects of the ac Josephson effect itself which would prohibit its practical application in this situation and also that absolute measurements of the frequency and voltage can be made with the required accuracy. The second question can be discussed either theoretically or experimentally, but the ultimate answer must rest on experimental evidence. In the absence of any theoretical evidence to the contrary, the Josephson frequency-voltage relation is presently thought to be theoretically exact. We have taken the view that a firmer foundation for a claimed determination of e/h can be laid by experimentally testing the invariance of the frequency-voltage ratio under a wide variety of experimental conditions. A demonstrated invariance at some level of precision constitutes strong circumstantial evidence that the ratio is equal to some fundamental physical quantity to that precision. The theoretical results can then be used with Occam's Razor to identify the fundamental quantity with $2e/h$. The invariance alone can be interpreted as evidence for the quantitative validity of the frequency-voltage relation at the demonstrated level of precision.

We may anticipate the conclusions to be drawn from the results reported here by stating that the answers to the first and second questions also turn out to be affirmative, i.e., a determination of the frequency-voltage ratio *can* be made at a useful level of accuracy and the ratio *can* reasonably be identified with $2e/h$. We have therefore attempted to describe the experiment and present the results in a manner appropriate to a report on the determination of a fundamental physical constant. This requires a more than ordinarily careful and detailed description of the experimental techniques and results so that independent judgments can easily be made of the possible sources of error and the validity of our result, as well as detailed comparisons with future redeterminations of e/h by this method. In Sec. II we discuss the physical ideas underlying the Josephson frequency-voltage relation in order to indicate the nature of the theoretical basis for confidence in the relation. This is followed by a description of the various types of weakly coupled superconducting systems in which the Josephson effects can be observed and a discussion of the experimental phenomena which provide access to the ac supercurrent. Section III contains a description of the apparatus and techniques used, and in Sec. IV the results are presented and discussed. Section V summarizes the conclusions which follow immediately from the results.[9] The final value of e/h that we obtain has a variety of far-reaching implications for the fundamental physical constants and for quantum electrodynamics. These are being analyzed in detail and will be presented in II.[8]

[8] B. N. Taylor, W. H. Parker, and D. N. Langenberg (to be published).

[9] Preliminary accounts of this work have appeared in W. H. Parker, B. N. Taylor, and D. N. Langenberg, Phys. Rev. Letters **18**, 287 (1967); D. N. Langenberg, W. H. Parker, and B. N. Taylor, in *Proceedings of the Third International Conference on Atomic Masses*, edited by R. C. Barber (University of Manitoba Press, Winnipeg, Canada, 1968).

II. ac JOSEPHSON EFFECT

A. Josephson Equations

The fundamental equations which describe the Josephson effects can be derived in a variety of ways,[6,10–12] all of which depend on the existence in a superconductor of a macroscopic phase-coherent quantum state. In the BCS theory this state is a consequence of a weak phonon-mediated attractive interaction which couples electrons together in bound pairs (Cooper pairs). The bound pair state is separated from the continuum of normal electron states by an energy gap equal to the binding energy of the pair. Because this interaction is weak, the average separation of the two electrons forming a pair is much greater than the average distance between electrons. This means that a given pair spatially overlaps perhaps a million other pairs. Under the restriction of the exclusion principle, the energetic advantage of condensation into the superconducting state is maximized if the center of mass momenta or, more generally, the quantum phases of the overlapping pairs are the same. In a bulk superconductor this locking of the pair phase is very strong and extends over macroscopic distances. This is the microscopic origin of the long-range order of the superconducting state envisioned by London.[1]

The Josephson effects arise when this phase locking is locally weakened. Conceptually, the simplest system to analyze is the tunnel junction treated by Josephson in his original work. Here two superconductors are separated by a thin insulating barrier. In the absence of a tunneling interaction between the two superconductors, the Hamiltonian is the sum of the Hamiltonians for metals 1 and 2:

$$H_0=H_1+H_2, \tag{2}$$

and the ground state of the system is the antisymmetrized product

$$\Psi_0=A\psi_0^{(1)}(N_1)\psi_0^{(2)}(N_2), \tag{3}$$

with energy

$$E_0=E_0^{(1)}(N_1)+E_0^{(2)}(N_2). \tag{4}$$

Here $\psi_0^{(1)}(N_1)$ is the ground state of superconductor 1 containing N_1 electrons and $\psi_0^{(2)}(N_2)$ is the ground state of superconductor 2 containing N_2 electrons. Now there is a large class of states obtained by transferring n electron pairs from superconductor 1 to superconductor 2:

$$\Psi_n=A\psi_0^{(1)}(N_1-2n)\psi_0^{(2)}(N_2+2n), \tag{5}$$

which are essentially degenerate with Ψ_0. The tunneling interaction lifts this degeneracy, giving rise to a phase-coherent linear combination of the Ψ_n. The details of this interaction depend upon the system being considered. For a weakly coupled tunnel junction the basic tunneling-interaction Hamiltonian[13] can be written[14]

$$H_T=\sum_{kq} T_{kq}(c_{k\uparrow}^{\dagger}c_{q\uparrow}+c_{-q\downarrow}^{\dagger}c_{-k\downarrow})+\text{H.c.} \tag{6}$$

Here $c_{k\uparrow}^{\dagger}$ creates an electron in a single-particle state of quasimomentum k and spin $\uparrow$ in metal 1 while $c_{q\uparrow}$ destroys a single-particle state with quantum numbers $q\uparrow$ in metal 2. The interaction is a one-body operator, and in order to transfer a pair it is necessary to go to second order. A straightforward calculation shows that (for identical superconductors)

$$(\Psi_m|H_T(E_0-H_0)^{-1}H_T|\Psi_n)=-\tfrac{1}{2}\pi^2N^2(0)|T|^2\Delta. \tag{7}$$

Here $N(0)$ is the single-spin density of states and Δ is the superconducting energy gap parameter. It is useful to express this matrix element in terms of a current I_1:

$$\hbar I_1/4e=\tfrac{1}{2}\pi^2N^2(0)|T|^2\Delta. \tag{8}$$

I_1 turns out to be equal to the current that would flow in the normal state of the junction at a voltage $\pi\Delta/2e$. Using this matrix element, standard degenerate-state perturbation theory then leads to the conclusion that the appropriate set of states in the presence of this coupling is[10]

$$\Psi_\varphi=\sum_n e^{in\varphi}\Psi_n, \tag{9}$$

with φ-dependent energies

$$E_\varphi=-(\hbar I_1/2e)\cos\varphi. \tag{10}$$

The parameter φ can be identified by considering what happens if the phase of the pairs on side 2 is shifted by θ relative to those on side 1. The Ψ_n transform as $\Psi_n\rightarrow e^{in\theta}\Psi_n$, so that $\Psi_\varphi\rightarrow\Psi_{\varphi+\theta}$, and we see that φ is the *relative* pair phase between superconductors 2 and 1. E_φ is thus a condensation energy associated with a phase-coherent coupling of the two superconductors and is minimized when the relative pair phase is zero (modulo 2π).

The energy change associated with the transfer of a pair is by definition equal to twice the electrochemical potential difference between the two superconductors. Therefore, in the presence of an electrochemical potential difference $\Delta\mu$, the state Ψ_φ evolves in time (to within an over-all phase factor) as

$$\Psi_\varphi(t)=\sum_n e^{in[(2\Delta\mu/\hbar)t+\varphi_0]}\Psi_n. \tag{11}$$

[10] R. A. Ferrell and R. E. Prange, Phys. Rev. Letters **10**, 479 (1963).

[11] B. D. Josephson, Rev. Mod. Phys. **36**, 216 (1964); Advan. Phys. **14**, 419 (1965).

[12] P. W. Anderson, in *Lectures on the Many-Body Problem*, edited by E. R. Caianiello (Academic Press Inc., New York, 1964), Vol. 2; in *Progress in Low Temperature Physics*, edited by C. J. Gorter (North-Holland Publishing Co., Amsterdam, 1967), Vol. 5.

[13] M. H. Cohen, L. M. Falicov, and J. C. Phillips, Phys. Rev. Letters **8**, 316 (1962).

[14] We assume that H_T has time-reversal symmetry, so that $T_{kq}=T_{k\uparrow q\uparrow}=T_{-q\downarrow-k\downarrow}$.

The tunneling current operator is

$$I=-(ie/\hbar)[H_T,N_1], \tag{12}$$

and to second order in the tunneling interaction the pair contribution to the current is

$$I=(\Psi_\varphi|I(E_0-H_0)^{-1}H_T+H_T(E_0-H_0)^{-1}I|\Psi_\varphi). \tag{13}$$

Using Eqs. (11) and (12), this expectation value can be directly evaluated. It is

$$I=I_1\sin\varphi, \tag{14}$$

with

$$\varphi=(2\Delta\mu/\hbar)t+\varphi_0. \tag{15}$$

If the electrochemical potential is varying in time, the rate of change of φ is given by

$$\partial\varphi/\partial t=2\Delta\mu(t)/\hbar. \tag{16}$$

If the relative electrochemical potential is due to a dc potential difference V, $\Delta\mu=eV$, then Eqs. (14) and (16) immediately yield an ac supercurrent with frequency given by the Josephson frequency-voltage relation $\nu=2eV/h$.

This brief outline of Josephson's theory illustrates the relevant physical factors. First, the state of the system consists of a phase-coherent linear combination of states which differ in the number of pairs transferred. This correlation is *enforced* by energy (or, at finite temperature, free-energy) considerations. Second, the time rate of change of the relative phases of the states forming this linear combination is determined solely by the electrochemical potential difference between the two superconductors. Since this is the essential feature upon which the interpretation of our experimental results rests, some further comments are in order.

The question immediately arises whether Eq. (16) is independent of the microscopic properties of the superconductors and of the mechanism that weakly couples the superconductors. The derivation outlined above makes use of the results of perturbation theory applied to a situation where the two superconductors are coupled by tunneling pairs. The calculation and the resulting form of the coherence energy, Eq. (10), and the current-phase relation, Eq. (14), are accurate only to second order in the tunneling interaction, but Eq. (16) is independent of the details of the perturbation calculation. It follows simply from the general time evolution of a quantum-mechanical wave function and the assumptions that the two isolated superconductors can be described by macroscopic quantum states Ψ_n and that coupling by any mechanism leads to a coherent superposition of states of different numbers of pairs similar but not necessarily identical to Eq. (9). These assumptions are strongly supported by the existence of flux quantization, by the elegant quantum interference experiments that have been performed by Mercereau and his colleagues, using multiple Josephson junction devices,[7] and, as we shall see, by the present experiments. It is probable that other coupling mechanisms would lead to different current-phase relations.[15] The pair current amplitude I_1 depends on tunneling matrix elements which in turn depend strongly on the properties of the insulating barrier and of the superconductors. It is temperature-dependent[16] and frequency-dependent.[17] It is reasonable to suppose, however, that, as long as the coupling is "weak" in some sense, whatever the mechanism, a periodic relationship between the current and the phase will persist. All available experiments in a wide variety of Josephson junctions support this view.[7] This is all that is required of the current-phase relation in the present experiments.

A second question is whether the factor 2 in Eq. (16) is generally valid. The time rate of change of the relative phase depends on the relative electrochemical potential, i.e., the change of the energy with number transfer (not charge transfer), and the factor 2 was inserted because we envisioned transfer of electron pairs in a manner consistent with the BCS theory. Higher-order processes involving coherent transfer of other numbers of electrons are conceivable; a process involving transfer of m electrons would lead to a frequency-voltage relation $\nu=meV/h$. As we shall see below, the strong nonlinearity of Josephson junctions, even those we believe to be adequately described by the simple equations (14) and (16), introduces various harmonic and subharmonic frequency effects which would render identification of any such higher-order processes virtually impossible. Indeed, the present experiment relies on these nonlinear effects. Consequently, as far as the determination of e/h is concerned, it really does not matter whether the factor is 2, so long as it is an integer. Processes involving the transfer of, say, $2+\epsilon$ electrons, where ϵ is of order 10^{-5}, cannot be excluded on *a priori* theoretical grounds. We do not feel competent to explore the theoretical basis for such a conjecture, but we believe that the consistency of the present results with other measurements of fundamental constants[8] renders this possibility unlikely on experimental grounds.

Two further questions can be discussed together. One is whether the presence of complex many-body interactions such as exist in both normal and superconducting metals might not lead to a renormalization of the effective charge of the electrons or pairs, just as they are known to renormalize the effective mass. This question has been raised in the past for normal metals[18] and largely laid to rest by experiment at the 0.1–1% level, but we are concerned here with possible effects at the part-per-million level. The other question concerns the

[15] B. B. Schwartz and A. Baratoff, Bull. Am. Phys. Soc. **12**, 76 (1967).

[16] V. Ambegaokar and A. Baratoff, Phys. Rev. Letters **10**, 486 (1963); **11**, 104(E) (1963).

[17] E. Riedel, Z. Naturforsch. **19A**, 1634 (1964); N. R. Werthamer, Phys. Rev. **147**, 255 (1966); D. J. Scalapino and T. M. Wu, Phys. Rev. Letters **17**, 315 (1966).

[18] See, for example, several papers in *The Fermi Surface*, edited by W. A. Harrison and M. B. Webb (John Wiley & Sons, Inc., New York, 1960).

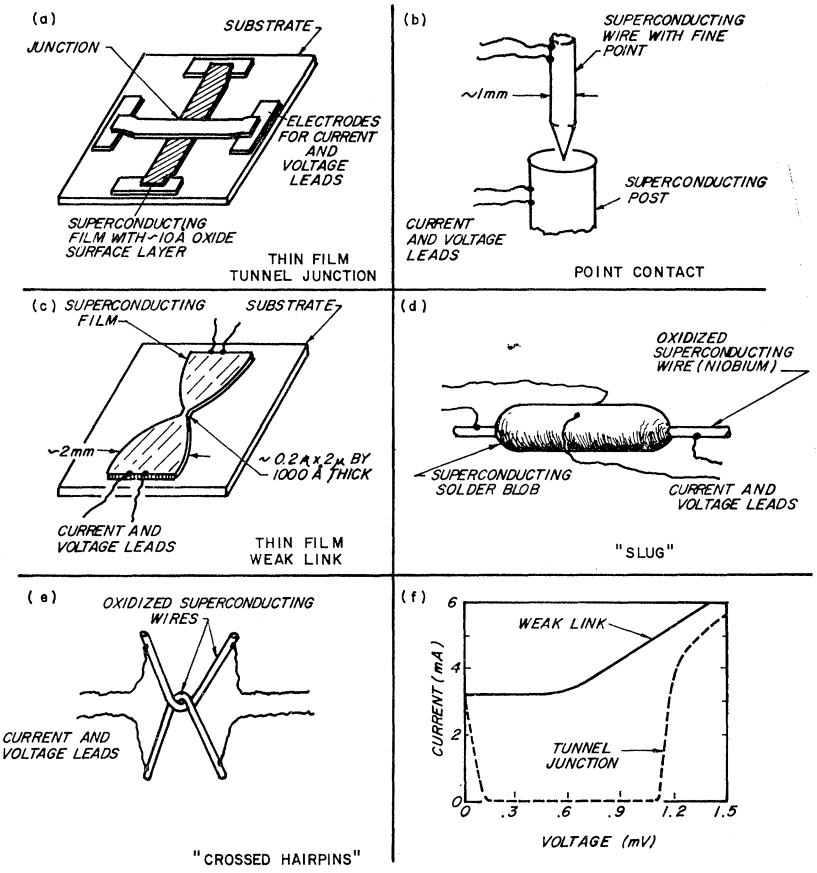

FIG. 1. Schematic diagrams of various types of Josephson junctions: (a) thin-film tunnel junction; (b) point contact; (c) thin-film weak link; (d) "slug"; and (e) "crossed hairpins." (f) Typical dc current-voltage characteristics for the two extreme types, the tunnel junction and the weak link.

effect of contributions to the relative electrochemical potential other than an electrostatic potential energy, e.g., contributions due to a temperature gradient, a stress gradient, a gravitational potential gradient, or a Bernoulli term.[19] The potential measurements reported here were made potentiometrically. We refer to them in the conventional way as "voltage" measurements, but in fact a potentiometer measures an electrochemical potential difference, and this forestalls all difficulties with these additional possible contributions to the potential. In a potentiometric measurement no current flows in the measuring circuit at balance because the net change in electrochemical potential around the circuit is zero. At balance, there exists across the terminals of the potentiometer an electrostatic potential difference V which is directly traceable, via a series of null balance measurements, to the operationally established absolute volt. If we imagine transferring a free electron from one potentiometer terminal to the other by any path whatever, we find that the energy change of the system is eV. The balancing procedure establishes that this energy change is precisely the same as the energy change involved in the transfer of a free electron from one terminal of the Josephson junction to the other. This latter energy difference is identically the electrochemical potential difference $\Delta\mu$ across the Josephson junction as *defined* above. Any complexities associated with the detailed behavior of the electron inside the junction simply do not enter, and we see that the appropriate charge is just the free-electron charge. If all potential differences in the external circuit except that at the Josephson junction are negligible, then $\dot{\varphi}=2\Delta\mu/\hbar=2eV/h$. In practice there are other potentials in the external circuit, like thermoelectric potentials, but these can be measured and corrected for.

Our purpose in presenting this discussion has not been to *prove* that the Josephson frequency-voltage relation provides an unassailable basis for a determination of e/h. As experimentalists, we may perhaps be pardoned some skepticism about the possibility of "proving" anything about the real world solely by theoretical arguments. We have instead attempted to convey a feeling for the generality of the arguments on which the frequency-voltage relation is based and to discuss some of the questions that we have had in mind while carrying out the experiments. We have tried to answer the questions experimentally by varying as many parameters of the system as possible and looking very carefully for changes in the result. In the end, our claim to a valid determination of e/h rests on the experimental results.

[19] J. Bok and J. Klein, Phys. Rev. Letters **20**, 660 (1968).

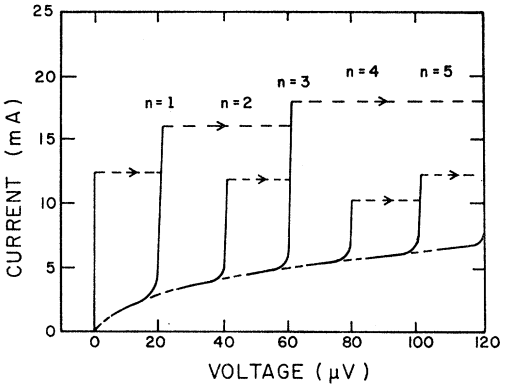

FIG. 2. *I-V* characteristic of a Sn-Sn oxide-Sn tunnel junction displaying self-induced current steps. The heights of the various steps depend on the externally applied magnetic field. Several field values were used to permit tracing out the steps shown.

Before concluding this section, we should remark for completeness that in the presence of a magnetic field derivable from a vector potential $\mathbf{A}(\mathbf{r},t)$, φ is to be replaced in the above equations with the gauge-invariant generalized quantity

$$\varphi-\frac{2e}{\hbar c}\int \mathbf{A}(\mathbf{r},t)\cdot d\mathbf{x}, \tag{17}$$

where the integral is taken across the junction.[7] The experimental confirmation of the many striking consequences of this are described in Ref. 7. Magnetic field is an important factor in the present experiments for various practical reasons but has no theoretically predicted or, as we shall show, experimentally observed effect on the validity of the Josephson frequency-voltage relation on which the experiments are based.

B. Josephson Junctions

As suggested in Sec. II A, the necessary and sufficient condition for a Josephson junction is some sort of weak coupling between two superconductors. This has been achieved in a variety of devices and Josephson effects are seen in all of them. Most of the more common devices are shown schematically in Fig. 1. Figure 1(a) depicts a thin-film tunnel junction of the type first used by Giaever for the study of single-particle tunneling in superconductors.[20] It is prepared by first evaporating a thin film of superconductor onto a substrate (usually glass) with preevaporated electrodes. Next, an oxide layer 10–20 Å thick is thermally grown on the surface of this film. The tunnel junction is completed by evaporating a second strip of superconductor over the top of the oxide layer. Figure 1(b) shows a structure known as a point contact.[21] It is made by forming a sharp point on a superconducting wire by some convenient method (mechanical polishing or chemical etching, depending on the material and the sophistication of the researcher) and pressing it against another superconductor. The contact pressure is quite critical, since it is the area of contact between the two superconductors which determines the strength of the phase coupling. The behavior of a point contact is usually similar to that of the simple weak-link structure shown in Fig. 1(c). This is composed of a single thin film with a constriction; the constriction is typically 2 μ wide and 0.2 μ long, and the film 0.1 μ thick.[22] Such junctions can be made by microscribing an evaporated superconducting strip or by evaporating through a suitable mask. Because of the large contact region compared with that of a point contact, thin-film weak links only behave as weakly coupled superconductors at temperatures close to the transition temperature of the superconductor. Figure 1(d) shows a device formed by freezing a blob of ordinary solder around a superconducting wire that has a naturally or artificially oxidized surface.[23] (This is called a "slug" because of the resemblance of the solder blob to that unsavory beast.) The behavior of this device usually indicates the presence of two or three separate localized Josephson junctions in the annular region between the solder blob and the wire. Figure 1(e) shows yet another way of achieving a point (or points) contact between two superconductors. Of these devices, the tunnel junction and the point contact were used in the present measurement of e/h.

The dc current-voltage (I-V) characteristics of tunnel junctions and weak links are compared in Fig. 1(f).[24] As the current is increased through a tunnel junction, no voltage is observed across the junction until the current reaches a certain critical value. [If there is no externally applied magnetic field and the self-field of the junction current is negligible, this maximum current is just the I_1 of Eq. (14).] When the critical current is exceeded, a finite voltage appears across the tunnel junction and it switches along the circuit load line to the normal (single-particle) I-V curve. At temperatures low compared with the transition temperature and for voltages less than $2\Delta/e$, where Δ is the superconducting energy gap parameter, the single-particle tunneling current is very small because there are few normal electrons available to carry the current. At a voltage equal to $2\Delta/e$, the energy available from the bias voltage becomes sufficient to break up the pairs and the tunneling current of normal electrons increases sharply as shown.

The mechanism for current flow in weak-link structures is not simply electron tunneling, since there is a continuous metallic path from one superconductor to the other. However, if the contact area is sufficiently

[20] I. Giaever, Phys. Rev. Letters **5**, 147 (1960).
[21] J. E. Zimmerman and A. H. Silver, Phys. Rev. **141**, 367 (1966).
[22] For a good discussion of the ac Josephson properties of thin-film weak links, see A. H. Dayem and J. J. Wiegand, Phys. Rev. **155**, 419 (1967).
[23] J. Clarke, Phil. Mag. **13**, 115 (1966).
[24] For a general review of some properties of tunnel junctions, see M. D. Fiske and I. Giaever, Proc. IEEE **52**, 1155 (1964).

small, Josephson effects are observed. At zero voltage a dc supercurrent again flows until a certain critical value is reached. The device then switches to the I-V curve characteristic of the constricted portion of the weak link in the normal state. The absence of a sharp increase in current at the gap voltage of the superconductor indicates that tunneling is not the dominant process taking place in these structures.

C. ac Josephson Phenomena

There are several experimentally observable phenomena which provide access to the ac Josephson supercurrent. One of these is the emission of radiation by the oscillating supercurrent. In a tunnel junction, radiation emission is closely associated with the appearance of self-induced steps in the I-V characteristic.[25] Figure 2 shows an example of the self-induced steps in a tunnel junction. These current steps result from the excitation of the resonant electromagnetic modes of the tunnel junction by the ac supercurrent. The resonant frequencies of a tunnel junction, viewed as an open-ended parallel plate transmission line, are given by $\omega_n = n\pi\bar{c}/L$, where L is the length of the junction, $\bar{c}$ is the phase velocity for propagation of electromagnetic waves in the junction, and n is an integer. Because the rf magnetic field penetrates into the superconductors with a penetration depth of several hundred angstroms, while the rf electric field is confined to the insulating barrier, $\bar{c}$ is considerably less than the velocity of light.[26] A typical value is $c/20$, so that the first resonant mode occurs at a frequency of 10 GHz (a convenient microwave frequency) for a junction about 0.8 mm long. If the voltage is adjusted so that the Josephson frequency matches the frequency of one of the resonant modes, the ac supercurrent couples strongly to the electromagnetic fields of the mode. The rf voltage induced across the junction reacts on the supercurrent, resulting in an excess dc current which appears as a current step in the I-V characteristic. Since $2e/h$ is approximately 500 MHz/μV, a voltage of 20 μV gives a Josephson frequency of 10 GHz. The interval between steps for a 0.8-mm-long junction should therefore be about 20 μV, as shown in Fig. 2. The effect of an externally applied magnetic field implied by Eq. (17) is to modulate the junction supercurrent density periodically in space.[7] The coupling of the ac supercurrent to a given mode can therefore be controlled by applying a magnetic field in the plane of the junction and normal to the dimension L.[25] When the junction is biased on one of these resonant modes, the electromagnetic fields within the junction

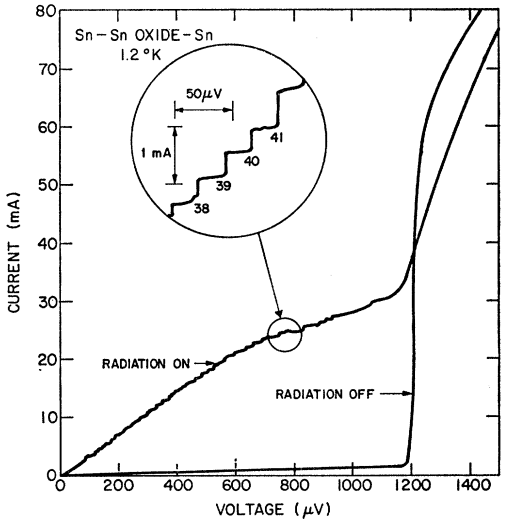

FIG. 3. I-V curves of a Sn-Sn oxide-Sn tunnel junction displaying radiation-induced current steps.

are maximized and the maximum power is radiated.[27,28] At present the observed radiated power is small, typically 10^{-11} W, and sensitive detection techniques are required. The voltage corresponding to 10 GHz is only 20 μV—too small to measure sufficiently accurately for a determination of e/h. However, experiments have shown that 10-GHz radiation is generated not only when the junction is biased on a mode resonant at 10 GHz, but also when it is biased on higher- or lower-order modes.[28] This subharmonic and harmonic radiation results from the nonlinear behavior of the junction when the rf voltage in the junction becomes comparable with the dc bias voltage. Analysis shows that this experimental result is consistent with the Josephson equations for a tunnel junction.[28,29] This subharmonic radiation phenomenon can be used to increase the voltage to be measured by an order of magnitude. It has been shown that a point-contact junction will also radiate if coupled to an external microwave resonator to provide the necessary resonant feedback.[30]

A second phenomenon which can be used to measure the frequency of the ac supercurrent was suggested by Josephson[6] and first observed by Shapiro.[31] The technique is to zero-beat the ac supercurrent with an applied microwave field and observe the resulting structure in the I-V curve of the junction. The effect arises essen-

[25] M. D. Fiske, Rev. Mod. Phys. **36**, 221 (1964); D. D. Coon and M. D. Fiske, Phys. Rev. **138**, A744 (1965); R. E. Eck, D. J. Scalapino, and B. N. Taylor, in *Proceedings of the Ninth International Conference on Low-Temperature Physics, Columbus, Ohio*, edited by J. D. Daunt *et al.* (Plenum Press, Inc., New York, 1965).

[26] J. C. Swihart, J. Appl. Phys. **32**, 461 (1961).

[27] I. K. Yanson, V. M. Svistunov, and I. M. Dmitrenko, Zh. Eksperim. i Teor. Fiz. **48**, 976 (1965) [English transl.: Soviet Phys.—JETP **21**, 650 (1965)].

[28] D. N. Langenberg, D. J. Scalapino, B. N. Taylor, and R. E. Eck, Phys. Rev. Letters **15**, 294 (1965); D. N. Langenberg, D. J. Scalapino, and B. N. Taylor, Proc. IEEE **54**, 259 (1966).

[29] N. R. Werthamer, Phys. Rev. **147**, 255 (1966); N. R. Werthamer and S. Shapiro, *ibid.* **164**, 523 (1967).

[30] A. H. Dayem and C. C. Grimes, Appl. Phys. Letters **9**, 47 (1966); J. E. Zimmerman, J. A. Cowan, and A. H. Silver, *ibid.* **9**, 253 (1966).

[31] S. Shapiro, Phys. Rev. Letters **11**, 80 (1963); S. Shapiro, A. R. Janus, and S. Holly, Rev. Mod. Phys. **36**, 223 (1964).

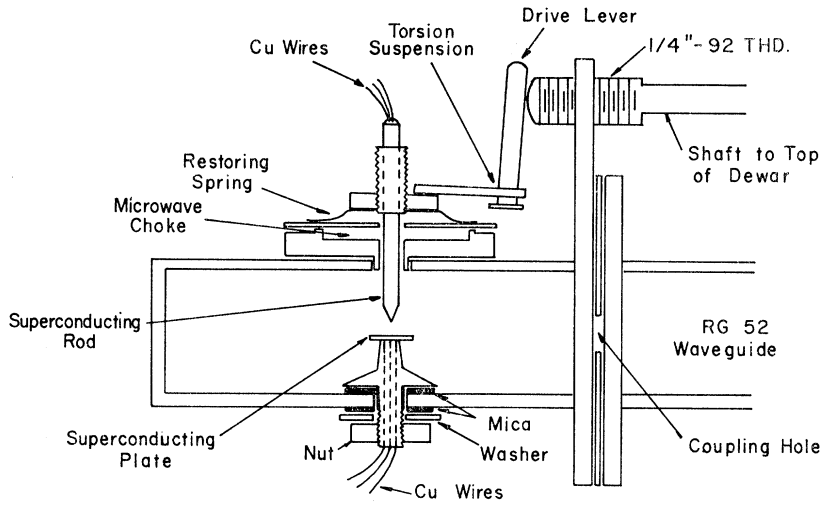

FIG. 4. *X*-band resonant cavity for point contacts.

tially from the time dependence of the vector potential in Eq. (17), but can be understood in the following way. When a junction is placed in a microwave field with angular frequency $\omega=2\pi\nu$, an rf voltage $v\cos(\omega t+\theta)$ is induced between the two superconductors. The total voltage across the junction including the dc voltage V is then

$$V+v\cos(\omega t+\theta). \tag{18}$$

From Eq. (16)

$$\dot{\varphi}=(2e/\hbar)[V+v\cos(\omega t+\theta)] \tag{19}$$

and

$$\varphi=2eVt/\hbar+(2ev/\hbar\omega)\sin(\omega t+\theta)+\varphi_0. \tag{20}$$

From Eq. (14)

$$I=I_1\sin[2eVt/\hbar+(2ev/\hbar\omega)\sin(\omega t+\theta)+\varphi_0]. \tag{21}$$

Expanding in Bessel functions,

$$I=I_1\sum_{n=-\infty}^{\infty}(-1)^nJ_n\left(\frac{2ev}{\hbar\omega}\right)\sin\left(\frac{2eVt}{\hbar}-n\omega t-n\theta+\varphi_0\right). \tag{22}$$

When $2eV/\hbar=n\omega$, the current has a dc component given by

$$I_{dc}=I_1(-1)^nJ_n(2ev/\hbar\omega)\sin(\varphi_0-n\theta). \tag{23}$$

This current may be varied between the limits $\pm I_1J_n(2ev/\hbar\omega)$ while the dc voltage remains constant. Thus, at a series of dc voltages $V_n=nh\nu/2e$, an excess current in the form of a sharp step will appear in the *I-V* curve of the Josephson junction. A measurement of the frequency of the applied microwave radiation and the voltage at which a current step occurs gives a value for e/h. [In the presence of a dc magnetic field Eq. (22) is modified by the addition of a multiplicative field-dependent Fraunhofer factor: The magnetic field thus affects the amplitude of the induced steps but not their position.]

Figure 3 shows the dc *I-V* characteristic of a Sn-Sn oxide-Sn tunnel junction irradiated with 10-GHz microwaves. The bottom curve was taken at zero applied microwave power and is a typical *I-V* curve for a superconducting tunnel junction (the dc Josephson current at zero voltage has been suppressed with a small magnetic field). The other curve was taken with microwave power applied. The portion of the *I-V* characteristic in the small circle is enlarged at the top of the figure and clearly shows the constant-voltage current steps. The numbers under each step are the integers in the generalized Josephson frequency-voltage relation $2eV_n=nh\nu$.

Microwave-induced steps similar to those in tunnel junctions are also observed in point contacts and weak links.[22] In these systems it is quite common to see steps at subharmonic voltages in addition to the harmonic voltages, i.e., at voltages given by $2emV_{nm}=nh\nu$, where both m and n are integers. As noted earlier, the current-phase relation (14) is a result of a perturbation calculation for a tunnel junction, so that it may not be the current-phase equation appropriate to a point contact or weak link. No detailed calculations have been made for such structures but the result should be $I=f(\varphi)$, where f is an antisymmetric periodic function with period 2π.[15] In the presence of a microwave field, the current would then be given by

$$I=f[2eVt/\hbar+(2ev/\hbar\omega)\sin(\omega t+\theta)+\varphi_0], \tag{24}$$

which contains harmonics of *both* $2eV/\hbar$ and ω. The mth harmonic of the Josephson frequency could beat with the nth harmonic of the applied radiation and produce the observed subharmonic steps.

Both of these effects—radiation emission and radiation-induced steps—thus involve a coherent microwave signal with a frequency related to a dc voltage by the simple relation $\nu=2emV_{nm}/nh$, where m and n are integers. Either could in principle be used to determine e/h. Unfortunately, we found in a preliminary study of

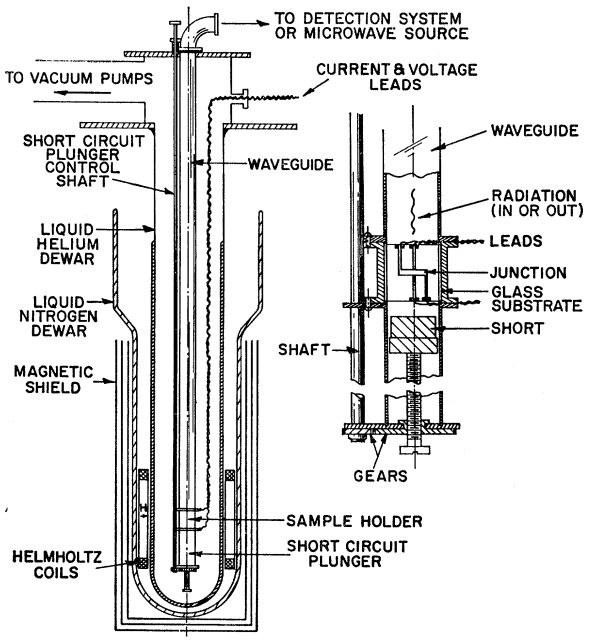

FIG. 5. Cryogenic equipment and X-band tunnel junction holder.

the Josephson frequency-voltage relation at the 60-ppm level[32] that, when tunnel junctions are biased on high-order self-induced steps, a new type of radiating mode is excited.[33] The detected radiation has a frequency that does not accurately satisfy the generalized frequency-voltage relation and depends strongly on the applied magnetic field. The appearance of this "non-Josephson" radiation limits the voltages that can be used in radiation emission experiments to relatively low values, and consequently limits the accuracy of the voltage measurements. We have therefore concentrated on the microwave-induced step phenomenon in the present experiments, although a few radiation emission measurements were made in order to check the basic equivalence of the two methods.

III. EXPERIMENTAL EQUIPMENT AND PROCEDURE

A. Josephson-Junction Preparation

Two types of Josephson structures were successfully used in these experiments: thin-film tunnel junctions and point contacts. The tunnel junctions were Sn-Sn oxide-Sn, Sn-Sn oxide-Pb, and Pb-Pb oxide-Pb. These were manufactured by evaporating 99.999%-purity Sn or Pb onto room-temperature glass substrates with preevaporated Ag electrodes. The pressure during evaporation ranged from as low as 10^{-7} up to 10^{-4} Torr with no obvious differences in the quality of the tunnel junctions obtained. The usual oxidation procedure was to condense oxygen into a liquid-nitrogen trap and admit it into the evaporator for periods of 12 h to three days at 50°C or room temperature, depending on the desired oxide thickness. The low-temperature normal-state resistance of the tunnel junctions so produced ranged from less than 10 mΩ up to almost 1 Ω. The dimensions of the junctions used for measurements in X band (10 GHz) were 0.8×0.3 mm; the 0.8-mm dimension was such that the first self-induced step occurred at approximately 10 GHz. For measurements at 70 GHz the dimensions were 0.4×0.3 mm.

The point contacts consisted of a sharpened rod of some superconducting material mounted in such a way that it could be carefully brought into contact with a stationary, flat surface of another superconductor. The rod was usually either Ta or Nb and was about 0.050 in. in diam by 1 in. long. On one occasion, a Ta rod was coated with Sn to form a Sn point contact. These rods were sharpened by turning them on a lathe with a steel tool and using, in succession, a clean metal file, 400-grit polishing paper, 600-grit polishing paper coated with light machine oil, and a final polish against a glass microscope slide coated with machine oil. The taper on the rod was typically 20°–30° (half-angle) and the radius of the point was less than 10 μ as determined by the resolution of a 40-power microscope. After measurements had been made on a point contact, the point was found to be flattened to a circle 20–50 μ in diam. The flat surface against which this point was pressed was usually either a sheet of 3-mil Ta or a chip of single-crystal Nb_3Sn. On one occasion a Ta sheet was coated with Sn to complete a Sn-Sn point contact.

B. Waveguide Junction Holders

For measurements in X band the point contacts were mounted in the rectangular microwave cavity shown in Fig. 4. It was made from a length of RG-52/U copper-plated waveguide with a copper plate soldered to one end and a copper-plated brass plate with a coupling hole in the center at the other end. The length of the cavity, approximately 4.7 cm, was chosen so that the resonant frequencies of the TE_{102} and TE_{103} modes were 9.0 and 11.5 GHz, respectively. The point contact was located in the center of the cavity and could therefore be located in either a strong rf electric field or a strong rf magnetic field by selecting the proper mode. The superconducting sheet of Ta or single-crystal Nb_3Sn was soldered on the post in the cavity and the Ta or Nb point entered the cavity through a quarter-wave choke on the opposite broad wall. Six copper wires were soldered to the point contact: four leads for the usual four-terminal I-V measurements and the other two for the accurate voltage measurement. The latter were twisted, brought out of the Dewar through a small hole sealed with Duco cement, and connected directly to the potentiometer in order to reduce thermal emfs.

[32] D. N. Langenberg, W. H. Parker, and B. N. Taylor, Phys. Rev. **150**, 186 (1966).
[33] D. N. Langenberg, W. H. Parker, and B. N. Taylor, Phys. Letters **22**, 259 (1966).

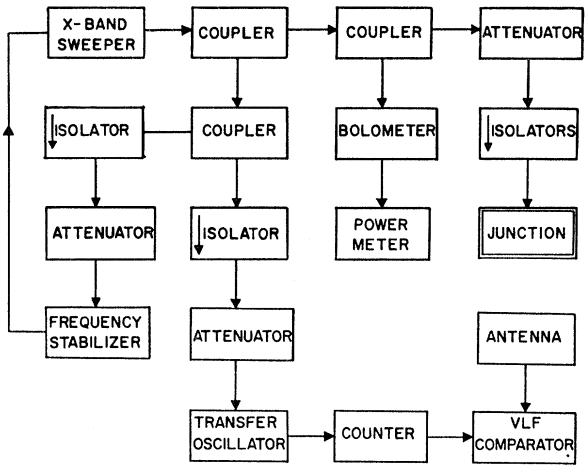

FIG. 6. Block diagram of X-band microwave system used to induce constant-voltage current steps.

On the right side of Fig. 5 is shown one of the sample holders used for measurements on tunnel junctions in X band. The tunnel junction was mounted in the waveguide with an adjustable short-circuit plunger below it for optimizing the coupling between the tunnel junction and the waveguide. In this junction holder the normal to the plane of the tunnel junction was perpendicular to the axis of the waveguide. Measurements were also made on tunnel junctions in another waveguide holder in which the normal to the junction plane was parallel to the waveguide axis. In this holder two different orientations were tried: one with the rf electric field parallel to the long dimension of the junction and perpendicular to the applied dc magnetic field and the other with the rf electric field perpendicular to the long dimension of the junction and parallel to the applied magnetic field. For the measurements at 70 GHz both the tunnel junctions and point contacts were mounted in a sample holder similar to that in Fig. 5 scaled down to the size of RG-98/U waveguide.

C. Cryogenic Equipment

Also shown in Fig. 5 is the cryogenic equipment used in these experiments. The Dewar system consisted of a standard set of glass liquid-helium inner Dewar and liquid-nitrogen outer Dewar. The helium Dewar was connected to a large mechanical pump through a 2-in. gate valve and a 4-in. pump line. The lowest temperature that could be reached was slightly less than 1.2K. One of two methods of temperature regulation was used when necessary. Below the lambda point, an electronic regulator, resistance bridge, and calibrated germanium thermometer were used. Above the lambda point, a needle valve and a Cartesian manostat (No. 8) connected in parallel with the main gate valve were used to control the pressure and consequently the temperature. The vapor pressure of the helium was measured using a mercury and/or oil (butyl-phthalate) manometer and converted to temperature using temperature–vapor-pressure tables for liquid helium.

D. Microwave Equipment

A block diagram of the X-band microwave system used to induce constant-voltage current steps is shown in Fig. 6. The microwave source used was a Hewlett-Packard (HP) 694D X-band (8–12.4 GHz) microwave sweep oscillator with a maximum output power of 30 mW or more at any frequency in X band. Part of this power (−10 dB) was coupled from the sweeper through an attenuator into a Curry, McLaughlin, and Len (CML) model MOS-1 microwave oscillator stabilizer which phase-locked the microwave oscillator to a quartz-crystal reference oscillator. When allowed to warm up for more than 8 h, this reference oscillator was stable to a few parts in 10^8 per hour. The frequency of the radiation was measured by coupling a portion of the power through an isolator and attenuator into a HP model 2590A microwave frequency converter and HP model 5245L electronic counter with HP model 5253B plug-in. The isolator was used to prevent spurious signals from the frequency converter from interfering with the frequency stabilizer. This frequency-counting system had a resolution of better than one part in 10^8. The reference time base of the counter was maintained to an accuracy better than one part in 10^8 by regular phase comparison (via a HP model 117A VLF comparator) with the U. S. frequency standard as broadcast by WWVB, Fort Collins, Colo. This phase comparison was made immediately before measurements of e/h on most junctions. With this equipment the average frequency of microwave radiation incident on the junction was known to better than one part in 10^8. A known portion of the microwave radiation could also be coupled into a bolometer in order to measure the amount of power incident upon the junction. A calibrated attenuator was used to vary the amount of power that reached the junction.

In Fig. 7 is shown a block diagram of the superheterodyne microwave receiver used to detect the radiation emitted by a tunnel junction in X band and to measure its frequency. The radiation entered the receiver through a HP model X362A low-pass filter and two isolators providing at least 70-dB attenuation of any local-oscillator signal leaking through the balanced mixer and 40-dB attenuation of the harmonics of the local oscillator generated by the crystals in the mixer. The local oscillator of this receiver was the HP sweep oscillator used with external amplitude leveling and the balanced mixer was a LEL model XFO-2 with integral 30-MHz preamplifier. The i.f. signal from the preamplifier was passed through a high-Q ($Q\sim500$) 30-MHz filter before being amplified by a LEL 30-MHz amplifier. To remove incidental FM and random changes in frequency, the local oscillator was phase-locked when high-accuracy frequency measurements were made. The frequency of the local oscillator was

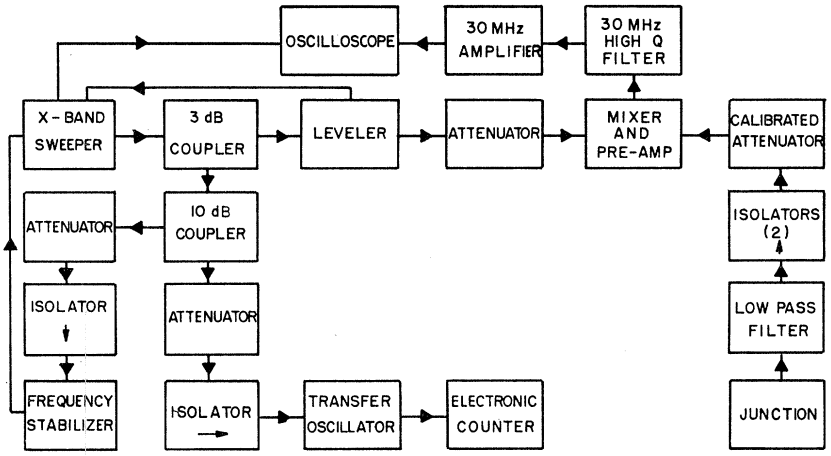

FIG. 7. Block diagram of X-band superheterodyne receiver.

measured with the electronic counting system previously described. In a superheterodyne receiver, the frequency of the detected radiation is $\nu_{LO}\pm\nu_{i.f.}$, or, if the i.f. bandpass is made very narrow by a high-Q filter, the frequency of the detected radiation is $\nu_{LO}\pm\nu_{filter}$. The frequency of the radiation was measured in this system by measuring the local-oscillator frequency and adding or subtracting, as appropriate, the center frequency of the filter. The latter could be measured to an accuracy of 2 kHz, yielding a net uncertainty of 0.2 ppm in the measured frequency.

Figure 8 is a block diagram of the microwave system used to induce constant-voltage current steps at 70 GHz. The 70-GHz signal was generated by an OKI 70V11A klystron. No attempt was made to phase-lock this klystron for two reasons. First, the residual FM of this klystron was only about 100 kHz, slightly greater than 1 ppm; second, the center frequency was exceptionally stable, changing by only a few ppm in several minutes. A special water-cooling jacket designed and built for this klystron contributed significantly to its frequency stability. A portion of the power (−10 dB) was coupled into a "home-made" harmonic mixer and generator (HMG) which made possible the accurate measurement of the frequency of the 70-GHz microwaves. In this device a phase-locked X-band signal whose frequency was accurately measured was harmonically mixed with the 70-GHz signal and a difference frequency at 30 MHz detected. The 30-MHz detector consisted of the high-Q filter and 30-MHz amplifier. The frequency of the 70-GHz radiation incident on the junction was then calculated using the equation

$$\nu=[(X\text{-band frequency})\times(\text{HMG harmonic number})]\pm\nu_{filter}. \quad (25)$$

In practice, the 70-GHz klystron was maintained at a constant frequency by "pulling" the klystron with an E/H tuner in order to keep the video output of the 30-MHz amplifier at a maximum.

E. Potentiometer

There are several reasons why it is important to give as complete a description as possible of the voltage-measuring system used in this experiment. First, *all* of the measurement uncertainty in this determination of

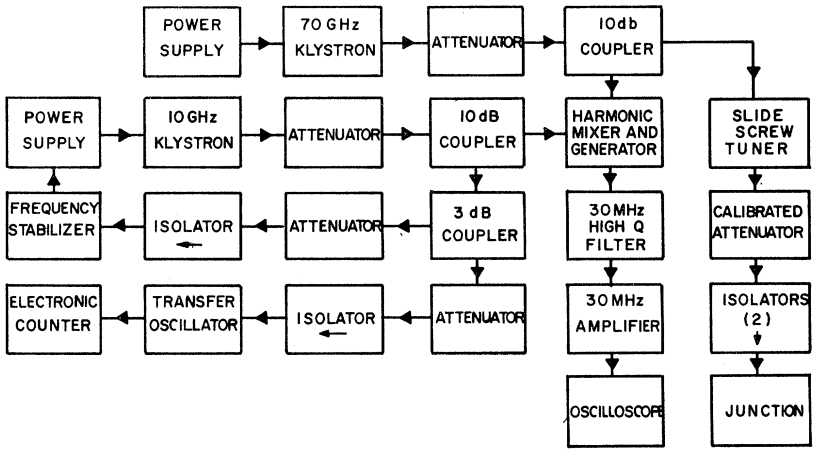

FIG. 8. Block diagram of 70-GHz microwave system used to induce constant-voltage current steps.

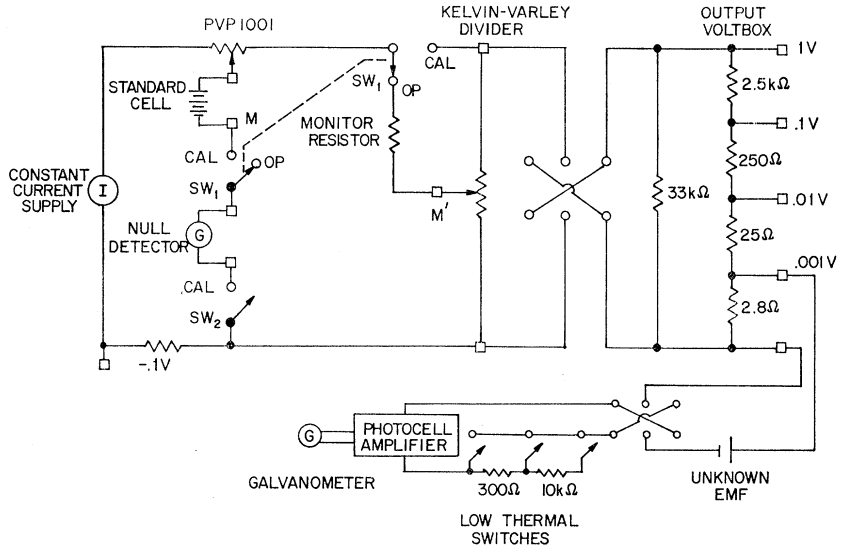

FIG. 9. Complete circuit of voltage-measuring system.

e/h resulted from limitations of the voltage-measuring system such as the uncertainty in the calibration and linearity of the potentiometer, resolution of the null detector, and stability and absolute calibration of the voltage standard. Second, the potentiometer used for these measurements appeared for the first time on the commercial market at about the time that these experiments were begun and therefore did not have a long history of proved reliability and accuracy. It therefore had to be demonstrated that this instrument performed in practice as well as the design criteria indicated and the manufacturer claimed. As we shall see, the instrument and the procedures developed for its calibration represent almost an order of magnitude advance in the state of the art of high-accuracy low-level dc measurements. For these reasons this section will contain a detailed description of the voltage-measuring system and all of the techniques that have been used for calibration.

Figure 9 shows all the components of the voltage-measuring system. It consisted of a modified Julie Research Laboratories, Inc. (JRL) PVP 1001 nanovolt potentiometer incorporating a JRL Kelvin-Varley divider model VDR 106/7, a set of six saturated standard cells (Eppley No. 101) in a constant-temperature air bath (Eppley model No. 106), a JRL ND 106 microvoltmeter used for standardizing the potentiometer, and a nanovolt null detector composed of a Guildline type 9145A low-thermal switch, a Guildline photocell galvanometer amplifier type 9460, and a Leeds and Northrup galvanometer No. 2430 D.

The principle of operation of the JRL PVP 1001 nanovolt potentiometer can most simply be understood by considering the simplified circuit shown in Fig. 10.[34,35] The potentiometer consists essentially of a constant-current source, a seven-decade 100-kΩ Kelvin-Varley divider of better than 1 ppm linearity, and an output voltbox composed of stable precision resistors. A simple analysis shows that, for constant current into the sliding arm of the divider, the current through the output voltbox (and hence the output voltage) is proportional to the divider setting. With the divider set at full scale, exactly 1 V can be established across the output resistors by adjustment of the constant current and comparison with a calibrated standard cell in the conventional manner. The output voltbox is provided with taps so that a series of decade ranges is available, the lowest range being 1 mV full scale. Once 1 V has been established across the output voltbox and the ratio of the decade resistors measured, a 1-mV full scale potentiometer with the stability and linearity of the current source and divider, respectively, has been realized.

An important feature of this potentiometer is that it is entirely self-calibrating, i.e., it has provisions that enable the operator to measure all factors which contribute to the accuracy of a voltage measurement and to make any necessary corrections. One such self-checking feature is provided to ensure that the standardizing resistors are accurate and that there has been no operator error in adjusting these resistors to the standard-cell value.[36] A 0.1–1.1-V range is established by the addition of a fixed resistor in series with the current supply (resistor at the −0.1-V terminal in Fig. 9). After standardizing the potentiometer in the conventional manner, the standard cell in series with a null detector is connected to the 1- and −0.1-V potentiometer terminals. If exactly 0.1 V appears across this resistor, then the value of the standard cell measured as an unknown on this range should agree with the value dialed into the standard-cell resistors. If not, the

[34] L. Julie, IEEE Trans. Instr. Meas. **IM-16**, 187 (1967).
[35] A. Abramowitz, Rev. Sci. Instr. **38**, 898 (1967).
[36] L. Julie, Electron. Instr. Digest **1**, 52 (1965).

standardizing resistors are in error and a correction must be applied to the measured value of any unknown voltage. The correction, if any, to the voltage across the 0.1-V resistor can be determined by measuring any constant voltage less than 1 V on both 1- and 1.1-V ranges. Any difference between the measured value of this constant voltage on the two scales is then the correction which must be applied to the 0.1–1.1-V scale. Using this procedure, it was demonstrated that the potentiometer standardization was accurate within ± 1 ppm.

An alternative method was used to reduce this uncertainty to ± 0.5 ppm. In this method, after standardizing the PVP 1001, a second potentiometer in series opposition with the standard cell was connected to the 1-V range. The PVP 1001 was set at full scale and the second potentiometer adjusted for null. The voltage at the terminals of the second potentiometer should then be equal to the emf of the standard cell minus exactly 1 V. This difference voltage (which could be measured to a high degree of accuracy with the PVP 1001) plus exactly 1 V should also equal the value set into the standardizing dials of the PVP 1001. Using this method, it was verified that the potentiometer was accurately standardized to within ± 0.5 ppm.

Another self-checking feature built into the potentiometer was used to verify that the operating current remained constant to better than 1 ppm as the divider setting was varied. This is important, since the impedance seen by the constant-current source varies from approximately 2.5 kΩ with the divider set at zero to approximately 28 kΩ with the divider set at midscale. The monitor resistor (see Fig. 9) is chosen so that approximately 1 V appears across this resistor when the operating current passes through it. With the null detector connected between terminals M and M' and SW_1 in the OP position, the null detector should show no change in deflection as the divider setting is changed if the current is truly constant. Using this procedure, it was verified that the operating current remained constant to better than 0.5 ppm as the impedance seen by the constant-current source was varied from maximum to minimum.

The linearity of the potentiometer depends on the linearity of the Kelvin-Varley divider as well as the constancy of the operating current. Techniques exist for the calibration of a Kelvin-Varley divider at a considerable number of dial settings, each equal to the ratio of two small integers. Using one of these techniques, known as the k/n method,[37] it was possible to calibrate the divider at up to 33 different dial settings. The maximum error was found to be only 0.3 ppm of full scale or an error of 3 digits on the seventh dial of the divider.

The major remaining accuracy-determining component of the potentiometer is the output voltbox. The

[37] L. Julie, *Notes on the Julie Ratiometric Method of Measurement* (Julie Research Laboratories, Inc., New York, 1964).

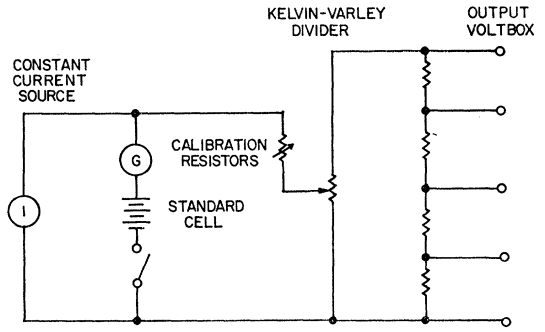

FIG. 10. Simplified schematic of nanovolt potentiometer.

voltbox is composed of four resistors with the nominal values 2.777778 Ω, 25 Ω, 250 Ω, and 2.5 kΩ. The resistors are oil-immersed in a hermetically sealed metal box. Using techniques developed by JRL[38] and the U. S. National Bureau of Standards[39] (NBS), the ratio of these resistors can be determined to high accuracy. The first method of calibration, and the one most often used, was to calibrate the 1/10 setting on the JRL VDR 106/7 Kelvin-Varley divider to measure the ratios at the terminals on the output voltbox. The first step in calibrating the voltbox was to construct a resistance ratio of nominal value 1/10 and accurately known to a few tenths of a ppm. This was done by measuring the values of 10 resistors, each nominally 10 kΩ, to 0.1 ppm in terms of a stable standard resistor using a high-resolution resistance bridge, the JRL PRB 205. The 10 resistors were the first 10 of 12 resistors in an oil-filled, hermetically sealed case (JRL DMR 105). The ratio of the first resistor to the series connection of all 10 resistors is then given by

$$r=R_1/\sum_{n=1}^{10} R_n=R_1/\sum_{n=1}^{10}(R_1+C_n)$$

$$=\tfrac{1}{10}\left[1-\tfrac{1}{10}\sum_{n=1}^{10}\frac{C_n}{R_1}+O\left(\frac{C_n}{R_1}\right)^2\right], \qquad (26)$$

where $C_n=R_n-R_1$. Any systematic error in the measurement of all of these resistors, even as large as 100 ppm, would produce less than 0.1-ppm error in the 1/10 ratio. The measurement uncertainty of 0.1 ppm for each of these resistors should result in a root sum square (rss) uncertainty in the ratio of slightly more than 0.1 ppm. In practice, however, the problem of self-heating prevented the realization of this high accuracy. As each resistor in the DMR 105 was measured, the power input slowly increased the temperature, so that the temperature of the DMR 105 when the tenth resistor was measured was not the same as when the first

[38] L. Julie, *A Ratiometric Method for Precise Calibration of Volt Boxes* (Instrument Society of America, Pittsburg, 1964).

[39] R. F. Dziuba and T. M. Souders, 1966 IEEE Int. Conv. Rec., Pt. 10, 1966.

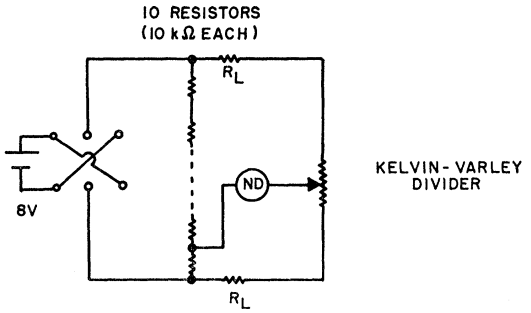

FIG. 11. Circuit for calibrating the Kelvin-Varley divider.

resistor was measured. Even though the rise in temperature and the temperature coefficient of the resistors were both small, the change in resistance could approach several tenths of a ppm. The result of several sequential measurements indicated that the uncertainty (70% confidence level) to be associated with the 1/10 ratio was approximately 0.5 ppm. The following procedure was used to correct for some of the changes due to self-heating: If the resistors were measured in order (1,2,···,10) and then immediately remeasured in reverse order (10,9,···,1), the average temperature for the two measurements of the nth resistor tended to be equal to the average temperature of the two measurements of all the other resistors. This procedure to some extent reduced the effect of both the self-heating of the resistors in the DMR and the reference resistor in the resistance bridge. As a result, the uncertainty in the value of the ratio as indicated by a series of measurements was reduced to about 0.3 ppm.

The calibrated 1/10 ratio was then used to calibrate the 1000000 and 099999(10) dial settings of the Kelvin-Varley divider (both settings must be calibrated, since some ratios in the voltbox were slightly greater than and some slightly less than 1/10). The simple circuit shown in Fig. 11 was used for this calibration. The Kelvin-Varley divider was calibrated to an accuracy of about 0.3 ppm of each dial setting, which required interpolating to 0.3 divisions on the seventh dial. It is important to realize that because of the resistance (approximately 3 mΩ) of the leads connecting the divider to the DMR 105, the divider was *not* calibrated at its input terminals but at the end of the leads. This introduced no error as long as the effective terminals of the divider were defined to be the ends of the leads and not the input terminals.

Using the calibrated Kelvin-Varley divider, the ratios at the voltbox terminals were then measured. The components were connected as shown in Fig. 12, where *all* the terminals on the PVP 1001 are carefully labeled. Also shown are typical values for the resistance of the internal lead wires for which corrections must be made. During the calibration of the 0.1- and 0.01-V ranges, the voltage which appeared across the resistors in the output voltbox was eight times the voltage across these same resistors during the actual operation of the potentiometer; during the calibration of the 0.001-V range, the voltage across the three smaller resistors in the voltbox was 80 times the voltage during actual operation. This increased heating was demonstrated in two ways *not* to produce any measurable systematic error. The voltage used during the calibration of the 1-mV range (the worst case of self-heating) was varied by a factor of 5 (power input by a factor of 25) with at most a 0.5-ppm change in the measured ratio. Secondly, the results of another calibration procedure (to be discussed shortly) which does not involve any self-heating problems agreed quite well with the results obtained using the procedure presently being discussed.

The final step of the calibration was to measure the lead resistance at the Galvo⁻, 0.01-, 0.1-, and 1-V terminals of the voltbox and to calculate the correction for this lead resistance. It was important to measure the lead resistance with all components connected so that any contact resistance was included in the measurement. Two techniques were used to measure the lead resistance and the results agreed to within 2 mΩ. One method utilized the *I-V* plotter used for sample biasing modified to operate as a milliohmmeter accurate to approximately 5% with a resolution of at least 1 mΩ. A second method is shown in Fig. 13. At null, the lead

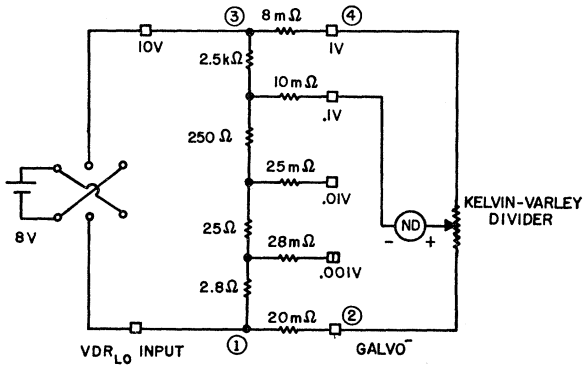

FIG. 12. Circuit for calibrating the output voltbox of the nanovolt potentiometer.

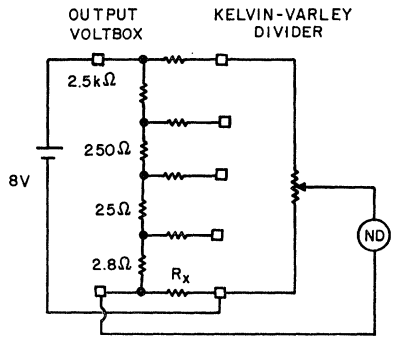

FIG. 13. Circuit for measuring the lead resistance.

resistance R_x is approximately given by

$$R_x = (2.8\ \text{k}\Omega) \times (\text{divider setting}), \qquad (27)$$

since R_x is small compared with 2.8 kΩ. All five leads could be measured in a similar way to an accuracy of 1 mΩ. In both these methods there was some ambiguity in the meaning of the lead resistance, because contact resistance made it impossible to locate exactly the effective end of the voltbox terminals. For this reason the lead correction was assigned an uncertainty of 0.3 ppm, approximately half due to measurement uncertainty and half due to ambiguity in the location of the effective voltbox terminals.

An alternative method of dealing with the lead resistance is to construct a network that will compensate for the resistance. A simplified circuit of the lead compensator is shown in Fig. 14. By the proper adjustment of R_1 the potential at terminals 1 and 2 can be made equal, and likewise with R_2 and terminals 3 and 4. The Kelvin-Varley divider then reads directly the ratio of the resistors in the PVP 1001 without the need for corrections due to the lead resistance. The difficulty with this method was that because of the limited resolution of the null detectors available, the lead compensator could not be balanced any better than the ratios could be measured (approximately 0.5 ppm). Experiments showed that complete calibrations with the lead compensator agreed within measurement error (0.5–1 ppm, depending upon the range) with complete calibrations making corrections for the lead resistance. This agreement suggests that the upper limit for any systematic error due to lead resistance was approximately 0.5 ppm per decade.

In an attempt to improve the accuracy of the potentiometer calibration, the following method was developed for transferring the synthesized 1/10 ratio directly to the PVP 1001, thereby bypassing the extra step of calibrating the Kelvin-Varley divider. The circuit on which this new method is based is shown in Fig. 15. A simple analysis shows that to better than 0.1 ppm the ratio of the resistors in the voltbox when

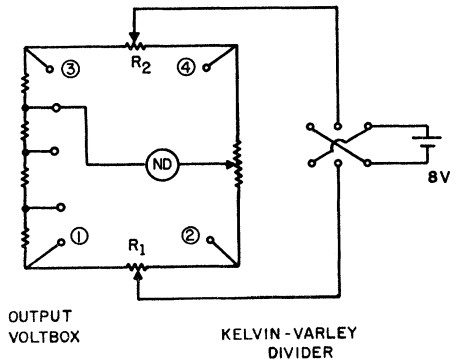

FIG. 14. Simplified circuit of the lead compensator.

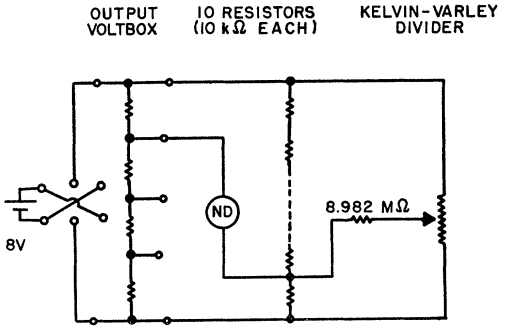

FIG. 15. Circuit for transferring 1/10 ratio directly to the output voltbox of the potentiometer.

the divider is adjusted for null is

$$1/10 + C + 1/1000(D - 1/10), \qquad (28)$$

where C is the correction to the synthesized 1/10 ratio and D is the divider setting (lead corrections were, of course, also necessary). This method has the advantage that the divider no longer measures the ratio but the deviation from 1/10, thus bypassing the need to interpolate on the seventh dial. There is also the advantage that only one measurement was required to transfer the 1/10 ratio to the voltbox and not the two measurements (divider calibration plus voltbox calibration) required with the previous method. The 8.982-MΩ resistor in Fig. 15 was a 8.94-MΩ resistor in series with a 100-kΩ variable resistor. The total resistance was adjusted to the correct value using the circuit in Fig. 16. The divider was set at 0.001 and the variable resistor adjusted for a null. A 9-kΩ resistor was added to simulate the internal resistance of the divider when connected as in Fig. 15. This process established the factor of 1/1000 in Eq. (28) to an accuracy of better than 0.1%. For a value of $D - 1/10$ five times larger than any correction encountered in practice, an error of 0.1% in the factor of 1/1000 would produce an error of only 0.1 ppm in the measured ratio.

The lead correction for this method was twice the lead correction of the previous method, because the loading on the voltbox was 50 kΩ, while with the first method it was 100 kΩ. This meant that twice the

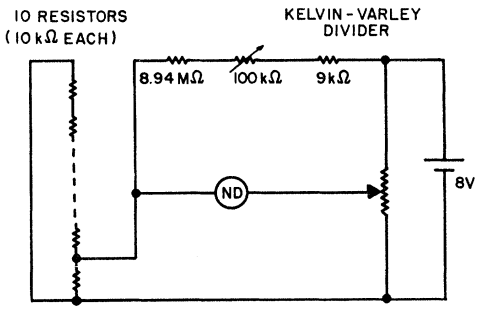

FIG. 16. Circuit for adjusting 8.982-MΩ resistor.

TABLE I. Comparison of methods of calibrating potentiometer.

PVP 1001 range	Result of ratio calibration of potentiometer (correction in ppm)	Result of voltage calibration of potentiometer (correction in ppm)
0.1 V	−4.5±1	−4.3±1
0.01 V	24.3±1.5	23.0±1.4
0.001 V	45.6±2	43.5±2

current flowed through the lead resistance, producing twice the voltage for which corrections had to be made. In practice this new method did not improve the accuracy of the over-all calibration, since any accuracy gained by avoiding the calibration of the divider was lost in the increased lead correction. However, it did provide an alternative method of calibrating the potentiometer, and thus contributed to the evidence indicating that there was no large systematic error in the calibration procedures. Experiments showed that this method of calibrating the output voltbox of the potentiometer agreed with the first method to approximately 0.3 ppm per decade.

Yet another and entirely independent method was also used to calibrate the potentiometer. This method was particularly useful because it used the potentiometer in the actual voltage-measuring mode rather than as a passive voltbox. Many of the problems associated with the previous methods such as self-heating and lead resistance were not present in this method. The procedure was to compare the value of a constant voltage measured on two different ranges and obtain the correction factor for the lower range necessary to bring it into agreement with the upper. For example, a voltage of approximately 99.99 mV could be measured on both the 1-V and 100-mV full-scale ranges. This constant 99.99 mV could be measured with 1-ppm *accuracy* on the 1-V range and with considerably better *precision* on the 100-mV range. [Recall that the Kelvin-Varley divider is a seven-decade divider, thus allowing 1-ppm resolution on the 1-V range. Also, the synthesized 1/10 ratio was used to calibrate the 099999(10) dial setting to approximately 0.5 ppm.] When the measured value of the voltage on the 1-V scale was compared with the measured value on the 100-mV scale, the correction factor was obtained with approximately 1-ppm uncertainty. Similarly, the correction to the 10- and 1-mV ranges could be obtained using constant voltages of 9.99 and 0.999 mV. The results of one such comparison of these two fundamentally different calibration methods are shown in Table I, where the uncertainties refer only to the uncertainty in calibrating the voltbox and neglect any uncertainty in the standardization. The uncertainties are rss and represent approximately a 70% confidence level. The excellent agreement is reassuring evidence that there was no large systematic error present in the calibration procedures. Although in principle this voltage calibration method is more straightforward than the ratio calibration, there are a number of practical limitations to its usefulness. The lack of an adjustable voltage source stable to 1 ppm required that this voltage frequently be interchanged between the two ranges being calibrated. This need for rapid measurements is incompatible with the requirements that the contacts come to thermal equilibrium and that thermal emfs be reduced to negligible size. In practice, the ratio calibration, although more complex in principle, could be performed more reliably in a reasonable length of time.

Even though there was good agreement among all the various procedures used to calibrate the PVP 1001, there is still the possibility of systematic errors in the measured value of an unknown emf. One possible source of such error is the shunting effect of leakage resistance to ground and the resulting currents which can flow in ground loops. Because of this possibility the leakage resistances were measured and the effect of the leakage current calculated. The result was that, while any individual leakage path would contribute a negligible error to the measurement of a voltage, the net effect of all the possible leakage paths could contribute as much as 1-ppm error to the measured value of e/h. Any such error can be shown to be in the direction which would increase the measured value of e/h.

The PVP 1001 potentiometer does not provide any resistance in series with the nanovolt null detector during the initial balancing. (On a standard potentiometer the sensitivity buttons select the series resistance. The highest sensitivity usually has no added series resistance.) Such resistance was necessary when the photocell amplifier was used as the nanovolt null detector, since the initial unbalance usually was sufficient to overload the amplifier considerably. To supply this series resistance, a Guildline low-thermal switch (five double-pole single-throw switches) was wired as both a sensitivity and reversing switch. Untinned solid copper wire was used throughout this switch. The switch was removed from its original thin Bakelite case and mounted in another built of $\frac{1}{4}$-in. aluminum plate to reduce temperature gradients across the switch contacts. Experiments showed that the remounted switch generated internal thermal emfs of less than 1 nV. This was accomplished by shorting the input terminals of the switch and connecting the output to a nanovolt detector. The detector indicated a change of less then 1 nV as the switch was changed from "normal" to "reverse" and back again. This low-thermal reversing switch in series with the null detector also eliminated the effect of thermal voltages in the null detector and doubled the effective sensitivity of the null detector. The noise level of the null detector limited the resolution to about $\frac{3}{4}$ nV.

F. Voltage Standard

Since a potentiometer is essentially a device which determines the ratio of two voltages, a standard voltage

TABLE II. Comparison of voltage at several bias positions on a radiation-induced current step for a Ta-Ta point contact.

Step No.	Position on step	Measured voltage (μV_L)	Change in voltage ΔV (nV)	Calculated voltage $V_{2e/h}$ (μV_L)	$(V_M - V_{2e/h})/\Delta V$[a]
18	Bottom Middle Top	447.56 447.66 ±0.01 447.74	180	447.675±0.002	−0.08±0.06
20	Bottom Middle Top	497.370 497.415±0.002 497.447	77	497.417±0.002	−0.03±0.04
20	Bottom Middle Top	497.367 497.412±0.002 497.442	75	497.417±0.002	−0.07±0.04
20	Bottom Middle Top	497.395 497.420±0.002 497.430	35	497.417±0.002	+0.09±0.08
12	Bottom Middle Top	298.416 298.426±0.002 298.438	22	298.422±0.001	+0.18±0.10

[a] V_M is the voltage at middle of step.

source traceable to the mksa absolute volt must be available in order to make absolute voltage measurements. In this experiment, the laboratory reference voltage was the mean voltage of a set of six saturated standard cells (Eppley model 101) calibrated by the NBS in terms of the U. S. legal volt as maintained by NBS. The conversion factor relating the NBS volt to the mksa absolute volt and the uncertainty in this conversion factor are discussed in Sec. IV B.

The uncertainty in the value of the local voltage standard referenced to the U. S. legal volt was due to any systematic change and/or calibration error in the emf of the six cells. The small random daily variations in the emf of 0.1 to 0.3 μV were essentially eliminated by frequent intercomparisons, but systematic changes in all six cells could not be eliminated by any means except a recalibration by NBS. Thus the standard cells were calibrated before (May–June 1966) and again after (July 1967) all the precision measurements had been completed. The results of these two calibrations revealed that the mean voltage of the six cells had increased 0.7 μV during the year in which the precision measurements were performed. The best value for the mean voltage during that year is therefore approximately 0.35 ppm larger than the mean of the earlier NBS calibration. All of our data were evaluated in terms of the first calibration and this will be referred to as our local volt V_L. In obtaining our final value for e/h in terms of the NBS volt we have applied a correction of −0.35 ppm, since the measurements were more or less uniformly distributed throughout the period between calibrations. We did not choose to interpolate linearly between calibrations and correct each run individually because the correction was relatively small compared with the possible systematic error in the calibration procedures followed by NBS. This has been estimated not to exceed 0.6 ppm.[40]

G. Experimental Procedure and General Observations

The procedure for the measurement of e/h using microwave-induced current steps was as follows. A Josephson junction, either a tunnel junction or point contact, was irradiated with sufficient microwave power to induce many steps as observed in the I-V curve of the junction. The amplitude and number of steps were optimized by adjusting the frequency of the applied radiation, the position of the microwave short, and the magnitude of applied magnetic field. After the appropriate steps had been induced, the microwave source was phase-locked and the frequency measured. The junction was then biased on one of the steps (usually at a voltage between 600 and 800 μV) and the voltage measured with the calibrated potentiometer. The current through the junction was immediately reversed and the voltage at which the same numbered step occurred was again measured. (The I-V curve was usually not quite symmetric about the origin, so that the current had to be slightly readjusted to remain biased on the same numbered step.) The value of e/h was calculated from the equation

$$2e/h = 2n\nu/(|V^+| + |V^-|), \tag{29}$$

where $|V^+|$ and $|V^-|$ were the magnitudes of the voltage of the nth step for the two different polarities. It was, of course, not necessary to use steps of the same order for both voltage polarities, or even integer-numbered steps. Quite often different-numbered steps for each voltage polarity and on several occasions

[40] U. S. National Bureau of Standards Report of Calibration Form No. NBS-5320.

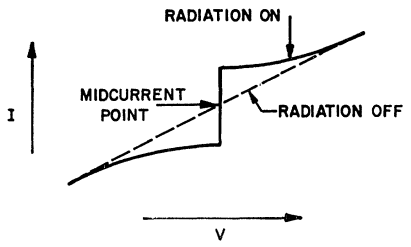

FIG. 17. Typical *I-V* curve of a radiation-induced current step observed with point contacts.

fractional-numbered steps (e.g., $21\frac{1}{2}$) were used; all gave the same value for e/h. Measurements at 70 GHz were made in an identical fashion except that the klystron was manually maintained at constant frequency as discussed in Sec. III D. The potentiometer was standardized at regular intervals throughout a series of measurements, but the operating current rarely had to be adjusted by more than 1 ppm at each standardization.

For most junctions, the voltage at which the step occurred was unique, i.e., there was no observable change in the voltage as the current was varied over the full height of the step. However, it was discovered that in both evaporated thin-film tunnel junctions and point-contact junctions with resistances of the order of 0.1 Ω and larger, the voltage was not truly constant as the current was varied on the steps. Since it was relatively easy to vary the resistance of a point contact, a study was made of these "nonvertical" steps using a Ta-Ta point contact. It was found that as the resistance was increased from 0.1 to 1 Ω, the voltage variation increased from 5 or 10 to as much as 200 nV. Absolute voltage measurements made at various positions on the step revealed that the voltage at the midcurrent point on the step gave a value of e/h equal within uncertainties to the average of all the data obtained on constant-voltage steps from other junctions. As the resistance was decreased (by increasing the pressure on the point contact), the voltage variation decreased but the midcurrent point continued to give a value of e/h in agreement with the constant-voltage step data. Extrapolating this behavior to point contacts with 5–10-nV voltage variation, it was assumed that the voltage at the midcurrent point was the correct value to insert into the Josephson frequency-voltage equation. All measurements on such steps were made at this midpoint.

Table II lists some of the data obtained on this Ta-Ta point contact. The expected voltage was calculated using the measured value of $2e/h$ (483.5978 MHz/μV_L), the measured frequency, and the potentiometer correction measured on the same day that the data were obtained. As seen from this table, the voltage at the midcurrent point agreed with the calculated voltage to within approximately 10% of the change in voltage on the step. Thus it seems reasonable to believe that with steps nonvertical by 10 nV or less, the midcurrent point occurs within 1 nV of the voltage at which the step would occur if it were of constant voltage.

An argument based on the simple treatment of induced steps given earlier suggests that the voltage at the midcurrent point on the induced step should be consistent with the Josephson frequency-voltage equation. Because of the existence of the phase term in the expression for the amplitude of the induced step [Eq. (23)] the step should be symmetric about the *I-V* curve of the junction in the absence of the microwave radiation. Figure 17 is a typical *I-V* curve of an induced step observed with point contacts and thin-film bridges.[22] The midcurrent point of the induced step is the point at which the junction would be biased if the Josephson effect did not exist. This point is thus stable against any noise voltage or thermal fluctuation which might cause the junction to switch from the induced step to the background *I-V* curve. At any other current and in the presence of fluctuations or noise voltages large enough to switch the junction off the induced step temporarily, the average observed voltage is no longer exactly equal to that consistent with the Josephson frequency-voltage relation, but is either larger or smaller depending on whether the junction is biased above or below the midcurrent point.

During the course of these measurements on induced steps, several observations were made concerning the response of Josephson junctions to externally applied radiation. In the case of point contacts in the *X*-band cavity it was found that microwave-induced steps were equally well induced at either resonant frequency of the cavity. Since at the lower frequency the point contact was positioned at a node of the electric field, while at the higher frequency it was at a node of the magnetic field, the equal response at either frequency suggests that the coupling between the ac Josephson current and the electromagnetic fields of the cavity is neither predominantly electric nor magnetic. For tunnel junctions, the coupling between the junction and the waveguide was strongest when the microwave short-circuit plunger was an odd number of quarter-wavelengths away and was essentially zero when the short was an integral number of half-wavelengths away from the junction. This suggests that the coupling to the resonant modes of a tunnel junction is via the electric field.

Although no careful investigation of the effect of orientation on the coupling between tunnel junctions and the waveguide was attempted, the general observation was that all three orientations (see Sec. III B) used did not differ in coupling by more than an order of magnitude, with the third (tunnel junction normal parallel to the waveguide axis and the waveguide electric field parallel to the applied magnetic field) possibly as much as an order of magnitude weaker in coupling than the other two orientations. The coupling depended on the position of the microwave short-circuit plunger in the same way for all three orientations. There was no obvious advantage, except for ease of

assembly, in using any one of these orientations for measuring e/h via either radiation emission or microwave-induced steps.

Steps were usually observed up to approximately $n=40$, corresponding to a voltage of about 800 μV, but radiation-induced steps were sometimes observed at voltages as high as 2.2 mV ($n\sim110$) in Sn-Sn oxide-Sn tunnel junctions. In such junctions the voltage Δ/e at which the energy of a Josephson-frequency photon becomes sufficient to break up an electron pair is about 0.6 mV. One might expect significant damping of the ac supercurrent by pair breaking to set in at this voltage. These observations, however, indicate that significant ac Josephson supercurrents still exist at frequencies nearly four times the frequency corresponding to the energy necessary to break up an electron pair.

The quality of the tunnel junctions used in these experiments varied from excellent to very poor. In an excellent tunnel junction, the single-particle tunneling current had the ideal form shown in Fig. 1(f). In a poor tunnel junction, the superconducting energy gap might be barely visible in the I-V curve, or it might be entirely absent and the I-V characteristic might resemble that of a weak link. This behavior was probably due to one or more small bridges of superconducting material piercing the oxide layer and directly connecting the two superconductors. However, even in the worst junctions, it was always possible to identify such ac Josephson effects as self-induced steps, microwave emission, and microwave-induced steps. Since these ac Josephson effects existed even in the most seriously bridged tunnel junction, each and every tunnel junction on which measurements on e/h were attempted yielded reliable data.

The measurement of e/h via microwave emission was made by biasing a tunnel junction on a high-order self-induced step and observing subharmonic radiation in X band. The applied magnetic field and the position of the microwave short were then adjusted for maximum emitted power. The local oscillator was phase-locked, and the junction voltage V was measured while the frequency of the emitted radiation was kept constant by continually readjusting the junction bias current. This frequency could be maintained constant to within 10 kHz without great difficulty. Immediately after the voltage measurements, the tunnel junction was biased in the dc Josephson mode and the residual voltage V_0 due to thermal emfs in the circuit was measured. The value of e/h was calculated from $2e/h=n\nu/(V-V_0)$. The frequency ν was measured as explained in Sec. III D.

The low-pass filter at the input of the microwave receiver (Fig. 7) was essential for the accurate measurement of the frequency of the emitted radiation. Without the filter, harmonics of the local oscillator generated by the crystals in the mixer could reach the tunnel junction and significantly alter the properties of the emitted radiation. Strange signals were then often observed, such as multiple sidebands (only two sidebands are expected in an ideal superheterodyne receiver), unequal sideband amplitudes, sidebands not separated by twice the i.f. frequency, and distorted line shapes.

Measurements of e/h via microwave emission were not made on self-induced steps higher than $n=6$ (approximately 120 μV), since all radiation detected from higher-numbered steps was identified as another type of radiation which we have called "non-Josephson" radiation.[33] Its characteristics are that its frequency is not precisely related to the voltage by the Josephson frequency-voltage relation and the frequency at a fixed voltage depends on external parameters such as magnetic field. There is no evidence to suggest that the non-Josephson radiation is a perturbation of the Josephson radiation. While the underlying mechanism is not known, all evidence to date is consistent with a nonlinear mixing of some sort of parametric oscillation within the junction with the rf fields driven by the ac Josephson supercurrent. There is no evidence of any effects related to this phenomena in the experiments on radiation-induced steps.

The linewidth of the emitted radiation did not limit the accuracy of the frequency measurements. The observed linewidths were typically a few kHz and corresponded to a spectral purity of a few parts in 10^7. This linewidth, like the finite slope of the radiation-induced steps, may be due to fluctuation processes within a tunnel junction.

H. Spurious Voltages

In making accurate low-voltage measurements, it is necessary to correct for or eliminate spurious voltages in the measuring circuit. Three possible sources of such spurious voltages were investigated: thermal emfs, Ohmic resistance within the four-terminal measuring network, and rectification of the microwaves and/or 60-Hz or rf pickup. The effect of voltages which did not reverse when the current was reversed (thermoelectric voltages, for example) was eliminated by measuring radiation-induced steps of both polarities. In one polarity the thermal emfs added to the voltage of the induced step, while in the opposite polarity they subtracted. Thermal emfs could be eliminated from the measurement in this way if they remained sufficiently constant during the measurement process. The thermal emfs were typically of order 100 nV and usually remained constant to better than 1 nV for a period of 1–2 min; this was quite long enough for the two necessary measurements. On the few occasions when the thermal emfs were changing significantly during the time required for the two measurements, the following averaging method was used. From a series of sequential measurements V_1^+, V_1^-, V_2^+, V_2^-, V_3^+, V_3^-, etc., the voltages used to calculate e/h were $\frac{1}{2}(V_1^+ + V_2^+) + V_1^-$, $\frac{1}{2}(V_1^- + V_2^-) + V_2^+$, etc. This method of averaging corrects for steady drifts if the voltage measurements were made at equal time intervals.

TABLE III. Values of $2e/h$ measured on Josephson junctions.

Run No.	Type of junction	Standard deviation of mean (ppm)	Potentiometer correction with random uncertainty (ppm)	Standard-cell correction (ppm)	$2e/h$ (MHz/μV_L)	Random uncertainty (ppm)
			A. Radiation-induced steps			
1	Sn-*I*-Sn	1	−30±10	···	483.5950	10
2	Sn-Sn	0.5	−29±5	···	483.5985	5
3	Ta-Ta	0.3	−37±1.7	−0.5±0.3	483.5984	1.8
4	Sn-*I*-Sn	0.3	−38±1.7	−0.5±0.3	483.5973	1.8
5	Sn-*I*-Sn	0.3	−41±1.7	−0.3±0.3	483.5960	1.8
6	Sn-*I*-Pb	0.5	−42±1.7	−1.0±0.3	483.5967	1.8
7	Nb-Ta	0.5	−42±1.7	−1.0±0.3	483.5989	1.8
9	Ta-Nb_3Sn	0.7	−44±1.7	+0.5±0.3	483.5977	1.9
10	Ta-Ta	1.2	−46±1.7	−0.4±0.3	483.5968	2.1
11	Sn-*I*-Pb	0.4	−43±1.7	+0.1±0.3	483.5983	1.8
		0.5	−24±1.7	+0.1±0.3	483.5995	1.8
12	Sn-*I*-Sn	0.3	−45±1.7	0.0±0.3	483.5976	1.8
13	Sn-*I*-Sn	0.7	−25±1.7	−0.1±0.3	483.5966	1.9
14	Sn-*I*-Sn	0.7	−38±1.7	+0.6±0.3	483.5982	1.9
		1.3	−21±1.7	+0.6±0.3	483.5985	2.2
15	Pb-*I*-Pb	0.25	−43±1.7	+0.4±0.3	483.5975	1.7
16	Sn-*I*-Sn	0.6	−39±1.7	+0.3±0.3	483.5983	1.8
17	Pb-*I*-Pb	0.3	−41±1.7	+0.3±0.3	483.5972	1.8
		0.3	−25±1.7	+0.3±0.3	483.5978	1.8
19	Sn-*I*-Sn	1.0	−39±1.7	+0.1±0.3	483.5972	2.0
20	Sn-*I*-Sn	0.5	−40±1.7	+0.8±0.3	483.5974	1.8
		0.5	−27±1.7	+0.8±0.3	483.5989	1.8
21	Ta-Ta	0.6	−42±1.7	+0.3±0.3	483.5978	1.8
Weighted average in terms of local volt (MHz/μV_L) (uncertainty is standard deviation of mean)						483.5978±0.4 ppm
			B. Radiation emission			
8	Sn-*I*-Sn	4	−44±1.7	−0.3±0.3	483.5991	4.4
18	Pb-*I*-Pb	5	−41±1.7	−0.3±0.3	483.5977	5.3
Weighted average in terms of local volt (MHz/μV_L)						483.5985±3.4 ppm
Weighted average of all data in terms of local volt (MHz/μV_L)						483.5978±0.4 ppm
Local volt to NBS volt correction						−0.0002
Final value of $2e/h$ in terms of NBS volt (MHz/μV_{NBS}) (uncertainty includes possible systematic error and is intended to be 1 standard deviation)						483.5976±2.4 ppm

Spurious voltages which reverse with current (e.g., Peltier emfs or those from Ohmic sources) were shown to be negligible by observing that the voltage in the measuring circuit was constant to within 1 nV over the full range of the zero-voltage currents arising from the dc Josephson effect. This eliminated any mechanism for producing a voltage between the two potentiometer leads which depends only on the existence of a current through the junction. Spurious voltages due to any rectification of the applied microwaves or 60 Hz and rf pickup were also shown to be negligible by several observations. First, the measured value of e/h was independent of microwave power over a range of 10 dB for a given junction and of 20 dB from junction to junction. Second, the measured value of e/h was independent of step number (see Sec. IV A), eliminating the possibility of an unknown source of constant voltage which did not increase as the current was increased. Finally, ac currents of frequencies from 60 Hz to 600 kHz and amplitudes many times greater than any observed pickup were deliberately introduced into the bias supply without any detectable change in the position of the microwave-induced steps. (Higher-frequency pickup signals would have produced a detectable splitting of the steps due to mixing of the pickup and applied microwave signals.[41]

IV. RESULTS AND DISCUSSION

A. Numerical Results

The results of 19 runs using radiation-induced steps and two runs using radiation emission are listed in Table III. The runs are numbered in chronological order; they were more or less uniformly distributed over the period August 1966 to May 1967. The type of junction used and the standard deviation of the mean of the measurements on each junction are given. Junctions of the form S_1-I-S_2 were thin-film tunnel junctions; I in each case was the oxide of S_1. Junctions of the form S_1-S_2 were point contacts. The potentiometer calibration correction listed is the average of the calibrations performed on the same day that the measurements were taken, usually one calibration before and one calibration after the measurements. The potentiometer uncertainty listed in the table represents an estimate only of the random errors in the calibration process. The decreased uncertainty after the first two measurements is the

[41] C. C. Grimes and S. Shapiro, Phys. Rev. **169**, 397 (1968).

result of improved calibration techniques. If two different potentiometer ranges were used on the same day, the results of measurements on both ranges were entered in the table. Also listed is the small correction due to changes in the emf of the standard cell used in the run because of small temperature changes of the air bath and random fluctuations in the emf of the cell as compared with the mean of all the cells in the local reference set. The values of $2e/h$ listed are referenced to the local voltage standard and the uncertainty in ppm is that due only to random errors. The possible systematic errors and the final experimental uncertainty are discussed in detail in Sec. IV B. In the remainder of this section we discuss the implications of the results given in Table III for the general validity of the Josephson frequency-voltage relation.

As noted in Secs. I and II, the strongest possible experimental evidence for the exactness of the Josephson frequency-voltage relation would be provided by a demonstration of the invariance of the measured frequency-voltage ratio under a wide variety of experimental conditions. Toward this end, we have looked for dependence of the measured frequency-voltage ratio on material, temperature, harmonic (step) number, voltage, microwave frequency and power, magnetic field, geometry, and microscopic mechanism responsible for the Josephson effect. We find that at the 2-ppm level of precision or reproducibility of the measurements the frequency-voltage ratio is independent of all these factors.

Measurements were made using five different superconductors (Sn, Pb, Nb, Ta, and Nb_3Sn) in various combinations in tunnel junctions and point contacts. These materials differ significantly in the microscopic parameters which are important in determining the properties of a superconductor, e.g., the energy gap, Debye temperature, density of states at the Fermi level, coherence length, London penetration depth, etc. An examination of Table III shows that measurements on all these materials resulted in the same value of the frequency-voltage ratio to within the 2-ppm precision of the measurements. For three of these materials (Sn, Pb, and Ta) there are enough data to allow application of a simple statistical test to see if the mean of the data on each material is indeed consistent within the experimental uncertainty. If the "t" test of significance between two sample means is applied to this data, it is found that the largest difference between two sample means—the results on Pb and Ta differ by 0.6 ppm—has a 55% probability of occurring by chance. This suggests the possibility that the Josephson frequency-voltage ratio may be material-dependent at the 0.6-ppm level. However, any such suggestion is highly speculative at this time, since the calculated standard deviation of the mean of *all* the measurements is 0.4 ppm.

The results of careful measurements of the frequency-voltage ratio as a function of temperature on two Sn-Sn oxide-Sn tunnel junctions are shown in Fig. 18.

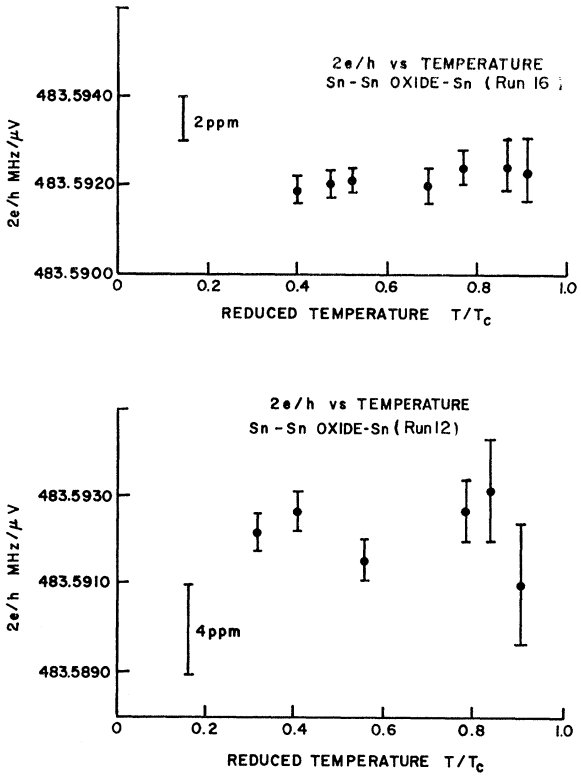

FIG. 18. Frequency-voltage ratio $2e/h$ versus temperature for two Sn-Sn oxide-Sn tunnel junctions.

The error bars represent only the standard deviation of the mean of the data at each temperature and do not include the uncertainty of the potentiometer calibration. To within the precision of these data (about 1 ppm) the Josephson frequency-voltage ratio is independent of temperature over the range $0.3 \leq T/T_c \leq 0.9$. Although induced steps were observed at higher temperatures, the steps were too small and unstable to permit biasing on a given one long enough to make an accurate measurement of the voltage. At a temperature $T/T_c = 0.9$, the superconducting energy gap is approximately half of its low-temperature value and $\rho = n_s/n$ (the ratio of the number of superconducting electrons to the total number of conduction electrons) is approximately one-third of its low-temperature value. Since changes in such parameters as the energy gap, superfluid density, and other material properties have no apparent effect on the numerical result, it is reasonable to assume that to within at least 1 or 2 ppm the Josephson frequency-voltage ratio is independent of the microscopic, solid-state properties of superconductors.

Since it was necessary to use high harmonics of the applied microwave frequency in order to obtain a voltage large enough to measure accurately, it was important to demonstrate that the generalized Josephson equation $2eV = nh\nu$ is valid independent of the value of n. In Fig. 19 are shown the results of measurements on a Pb-Pb oxide-Pb tunnel junction on a series

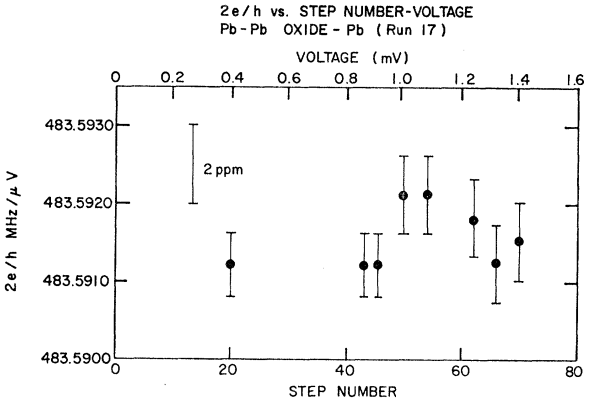

FIG. 19. Frequency-voltage ratio $2e/h$ versus step number and voltage for a Pb-Pb oxide-Pb tunnel junction.

of different steps. To within ± 1 ppm, the Josephson frequency-voltage ratio is independent of step number up to at least $n=70$. These data indicate that to within 1 ppm the frequency-voltage ratio is independent of the potential difference between the two superconductors over the range of a few hundred microvolts to approximately 1.5 mV.

Measurements have also shown that the frequency-voltage ratio is independent of microwave frequency and power. While most measurements were made at frequencies near 10 GHz (X band), runs 19 and 21 (see Table III) were made at 70 GHz. Data were taken on both a tunnel junction and a point contact. The average result obtained at 70 GHz (483.5975 MHz/μV_L) differs from the average of the X-band data (483.5978 MHz/μV_L) by about 0.6 ppm—well within the 2-ppm precision. A measurement of the frequency-voltage ratio as a function of microwave power on a Pb-Pb oxide-Pb tunnel junction demonstrated that a change of 10 dB produced no observable change in the result. The results of measurements on one step are given in Table IV.

The two types of junctions used for these measurements—tunnel junctions and point contacts—differ in two important properties: geometry and microscopic coupling mechanism. The evaporated thin-film tunnel junction displays observable structure in the I-V characteristic due to self-excitation of resonant junction modes.[25] The point contact, on the other hand, is nonresonant; there are no natural frequencies associated with geometric resonances, and no structure is observed

TABLE IV. Frequency-voltage ratio $2e/h$ at several microwave power levels.

Microwave power (mW)	$2e/h$ (MHz/μV_L)
20	483.5970±0.6 ppm
10	483.5970±0.6 ppm
2	483.5969±0.6 ppm

TABLE V. Comparison of data from tunnel junctions and point contacts.

Structure	$2e/h$ (MHz/μV_L)
Point contacts	483.5981±0.8 ppm
Tunnel junctions	483.5977±0.5 ppm

in the I-V characteristic unless the point is strongly coupled to an external resonator such as a high-Q microwave cavity. Even though other researchers have reported such structure,[30] we observed no such structure induced in the I-V characteristic by the cavity used in this experiment. Of more importance is the fact that the general derivation of the Josephson frequency-voltage relation indicates that this relation is independent of the microscopic processes responsible for the phase coupling between two superconductors. Electron tunneling is the microscopic coupling mechanism in thin-film tunnel junctions but is almost certainly not the mechanism responsible for the coupling in point contacts. In Table V are listed the average values of the frequency-voltage ratio measured on point contacts and tunnel junctions; the uncertainty is the standard deviation of the mean of the several measurements. The t test of significance between the two sample means shows that there is a 40% probability of the difference (0.6 ppm) occurring by chance. The results of the t test again suggest the possibility of a small (0.6-ppm) difference in the measured Josephson frequency-voltage ratio in point contacts and tunnel junctions. If it is real, this difference is not independent of the possible material dependence, because the point contacts usually were fabricated of type-II superconductors and the film junctions of type-I superconductors. However, as noted above, the existence of a real difference is highly speculative.

A change of magnetic field of magnitude 0 to ± 10 G produced no detectable change in the frequency-voltage ratio. Larger magnetic fields reduced the amplitude of the Josephson effects to a level where accurate measurements could no longer be made.

Measurement of the frequency of radiation emitted by the ac supercurrent provided a separate experimental method of measuring e/h. Measurements were made on tunnel junctions of two materials: Sn-Sn oxide-Sn and Pb-Pb oxide-Pb. The two results differed by less than 3 ppm, well within the uncertainty of approximately 5 ppm. Although the measurements were of relatively low accuracy because of the voltage limitation imposed by the non-Josephson radiation, the resulting mean value of the frequency-voltage ratio exceeds the mean value obtained by the method of radiation-induced steps by only 1.4 ± 3.4 ppm. The results of the two methods are compared in Table VI.

B. Final Result and Sources of Uncertainty

The fact that no significant changes in the frequency-voltage ratio were observed when the experimental

TABLE VI. Comparison of data obtained via radiation-induced current steps and radiation emission.

Method	$2e/h$ (MHz/μV_L)
Radiation emission	483.5985±3.4 ppm
Radiation-induced steps	483.5978±0.4 ppm

conditions and solid-state parameters were varied over wide ranges strongly implies that the ratio is indeed equal to a fundamental physical constant. Guided by the theoretical considerations discussed in Sec. II, we identify this constant as $2e/h$. The average of all the data in Table III weighted as the inverse squares of the random uncertainties is $2e/h = 483.5978$ MHz/μV_L. The 1 standard-deviation uncertainty due to random error alone is 0.4 ppm.

The sources of uncertainty in the final value of e/h as measured in terms of the NBS volt are summarized in Table VII. The 0.01-ppm uncertainty in the frequency measurement makes a negligible contribution to the final uncertainty. The random uncertainty of 0.4 ppm in the measurement of the voltage is the result of three contributions: one from the measurement process itself, one from the potentiometer calibration, and one from fluctuations in the emf of the standard cells. An estimate of the random error in the measurement process due to the 1-nV resolution of the null detector, drift of the thermal emfs in the circuit, and the stability and linearity of the potentiometer leads one to expect a standard deviation of approximately 1.5 ppm for a series of measurements on a given junction. The observed standard deviations of 1–3 ppm indicate that the random errors in the measurement process are understood. The *estimated* random error in the potentiometer calibration procedure is due to finite null-detector resolution and is approximately 1.5 ppm. An *experimental* method of determining the random error in the calibration of the potentiometer would be to measure an accurately reproducible voltage many times. Since the only available 1-mV signal source with the necessary reproducibility was a Josephson junction, the 1.7-ppm standard deviation of all of the induced step measurements listed in Table III represents the best available experimental evidence for the random error in the calibration process. This standard deviation of 1.7 is in satisfactory agreement with the estimated random uncertainty of 1.5 ppm. The random uncertainty σ_i assigned to the result of each run on a particular junction (last column of Table III) is the rss of the standard deviation of the mean of the measurements, the 1.7-ppm uncertainty in the potentiometer calibration, and the standard-cell uncertainty. The total random uncertainty $\sigma = 0.4$ ppm in the final value of e/h is then obtained from the equation $1/\sigma^2 = \sum_i 1/\sigma_i^2$.

To this random uncertainty must be added an estimate of the possible systematic errors. These arise from the several sources indicated throughout the text and listed in Table VII. The two contributions to the uncertainty of the value of the local voltage standard in terms of the NBS volt were discussed in Sec. III F. The possibility of a 0.5-ppm systematic error due to aging and changes of the emf during transportation of the standard cells is based on the observed 0.7-ppm increase in the mean emf of the standard cells during the year between calibrations by the NBS.

TABLE VII. Contributions to the uncertainty in the measured value of e/h (in units of ppm). All uncertainties are intended to be 1 standard deviation.

I. Frequency		0.01
II. Voltage		
(a) Random error	0.4	
(b) NBS calibration of standard cells	0.6	
(c) Transportation and aging of standard cells	0.5	
(d) Standardizing potentiometer	0.5	
(e) Establishing 1/10 ratio, 0.3 ppm, additive per decade	1.0	
(f) Lead-resistance correction, 0.3 ppm, additive per decade	1.0	
(g) Ground-loop currents	1.0	
(h) Stability of operating current	0.5	
(i) Self-heating during calibration	0.5	
(j) Linearity of divider	0.5	
(k) Temperature drift of output voltbox	1.0	
rss total		2.4

The possible systematic errors due to the potentiometer standardization, i.e., changes in operating current, ground-loop currents, and self-heating of the potentiometer output voltbox during calibration, were all discussed in detail in Sec. III E, where it was explained that a possible 0.3-ppm systematic error could exist both in establishing the 1/10 ratio and in determining the lead-resistance correction. Since three resistance decades must be calibrated in order to determine the correction to the 1-mV potentiometer range, each of these two uncertainties leads to a 1-ppm possible systematic error.

It was not uncommon to find the measured potentiometer correction after the precision measurements to be 2 or 3 ppm greater than the correction before the measurements and to find at the same time an increase in the ambient temperature of 2 or 3°C. This effect was probably due to a differential temperature coefficient of the resistors in the output voltbox of the potentiometer. Taking the average of the two calibrations reduced the effect of this temperature drift but could not eliminate it. An estimate of the systematic error introduced in this way is approximately 1 ppm.

As a possible over-all check on the accuracy of the calibration procedures, measurements of e/h were made on both the 1- and 10-mV ranges of the potentiometer on four occasions. Steps above 1 mV were induced in the two junctions measured in runs 11 and 17. Runs 13 and 14 were made using two Sn-Sn oxide-Sn junctions

evaporated on one substrate and connected in series in order to obtain a voltage larger than 1 mV. The average measured value of e/h on the 10-mV range was only 0.8 ppm higher than the average on the 1-mV range. The application of the t test indicates that there is approximately a 45% probability of the difference being this large or larger by chance. This suggests the possibility of a small systematic error of perhaps 0.5 ppm in the calibration of the 1-mV range in terms of the 10-mV range. An error of this magnitude is not unexpected in the light of the possible sources of systematic error listed in Table VII. On one occasion (run 20) another PVP 1001 was borrowed from JRL and measurements made with this instrument (also modified) were compared with the average value of e/h obtained with our own potentiometer. The results differed by 2.5 ppm. Since the total uncertainty including both random and systematic error in a single calibration of the potentiometer is approximately 3 ppm, this agreement is satisfactory. Both of the comparisons just discussed and the results of the various independent calibration procedures described in Sec. III E are all reassuring evidence that the uncertainties in Table VII are realistic estimates.

The rss of the random error and possible systematic error is 2.4 ppm. Applying the -0.35-ppm correction implied by the change in value of the standard cells during the 1-yr period of the measurements, our final value of $2e/h$ referred to the NBS volt is

$$2e/h = 483.5976 \pm 0.0012 \text{ MHz}/\mu V_{NBS} \text{ (2.4 ppm)}.$$

To convert this value to absolute units requires knowledge of the conversion factor relating the NBS volt to the absolute volt. The value of the NBS volt in mksa units is experimentally determined by passing one absolute ampere through a resistance of one absolute ohm and comparing the resultant emf with that of the national reference cells. Since voltages of essentially equal magnitude at the 1-V level can be compared to better than 1 ppm, the uncertainty in establishing one absolute volt is equal to the rss of the uncertainties in establishing the absolute ohm and ampere. On the basis of absolute ohm determinations at the NBS[42] and other national laboratories,[43] the value of the NBS ohm probably differs from the absolute ohm by less than 1 ppm. However, since the absolute ampere has been experimentally established to only about ± 6 ppm,[44] the necessary conversion factor from NBS volts to absolute volts can be directly determined to only 6 ppm—more than double the uncertainty of our measured value of e/h referenced to the NBS volt. This problem is not unique to our measurement of e/h. Many of the experimental determinations of fundamental physical quantities, such as the Faraday and the gyromagnetic ratio of the proton, are plagued with this problem of converting from "as-maintained" electrical units to the mksa system of units. In II,[8] where we critically analyze the role played by conversion factors, we find that the most reasonable solution to the probelm is to treat the ratio of the NBS ampere to the absolute ampere as an adjustable parameter in a complete least-squares adjustment of the fundamental physical constants. The result of that adjustment is

$$V_{NBS}/V_{ABS} = 1.0000088 \pm 2.6 \text{ ppm}.$$

Applying this conversion factor to our experimental result, we find that

$$2e/h = 483.5933 \pm 0.0017 \text{ MHz}/\mu V_{ABS} \text{ (3.6 ppm)}$$

or, in more conventional units,

$$h/e = (4.135707 \pm 0.000015) \times 10^{-15} \text{ J sec/C}.$$

The 3.6-ppm uncertainty quoted here was obtained by taking the rss of the 2.4-ppm uncertainty in our experimental result and the 2.7-ppm uncertainty in the voltage conversion factor. Strictly speaking, this procedure is not proper because these errors are correlated via the least-squares adjustment.[8] It does, however, allow us to put our result in a form which can be compared with the "best" value of h/e which results from the least-squares adjustment:

$$h/e = (4.135708 \pm 0.000014) \times 10^{-15} \text{ J sec/C}.$$

We would like to emphasize that the real direct result of the present experiment is a value of e/h referred to the NBS volt as it existed in 1966–1967. (If, as appears likely, the NBS redefines the U. S. legal volt so that it is closer to the absolute volt, the value quoted here for $2e/h$ in units of $\text{MHz}/\mu V_{NBS}$ will have to be corrected appropriately. (See note added in proof.)

V. CONCLUSIONS

The value of e/h obtained in the present experiments is 38 ± 10 ppm smaller than the value given by the Cohen-DuMond 1963 least-squares adjustment of the fundamental physical constants.[45] Since a difference exceeding three standard deviations has a very small probability of occurring by chance, it is reasonable to suppose that there is a large undetected systematic error in either this measurement of e/h (including the assertion that the Josephson frequency-voltage ratio is equal to $2e/h$) or in one or more input data of the 1963 adjustment. An adequate discussion of this discrepancy, its resolution, and the resulting implications for quantum electrodynamics and our knowledge of the fundamental physical constants can only be made within the

[42] R. D. Cutkosky, J. Res. Natl. Bur. Std. (U.S.) **65A**, 147 (1961).

[43] G. H. Rayner, Metrologia **3**, 11 (1967); A. M. Thompson, *ibid.* **4**, 1 (1968).

[44] W. J. Hamer, *Standard Cells, Their Construction, Maintenance, and Characteristics*, National Bureau of Standards Monograph No. 84 (U. S. Government Printing Office, Washington, D. C., 1965).

[45] E. R. Cohen and J. W. M. DuMond, Rev. Mod. Phys. **37**, 537 (1965).

context of a careful evaluation of all the existing experimental data related to the fundamental physical constants. This is done in II.[8] Here we confine ourselves to a discussion of our experimental results as they relate to the present theory of superconductivity and the questions raised in Sec. II A.

First, we must make it clear that this experiment is not as explicit a demonstration of the pairing concept in superconductivity as one might initially assume from the high accuracy of the measurements. There can be no doubt that to within the accuracy with which e/h is known from other experiments (about 40 ppm),[45] the charge on the fundamental current carrying entity in a superconductor is an exact multiple of the free-electron charge. However, the presence of harmonic and subharmonic effects resulting from the nonlinear behavior of a Josephson junction makes it impossible to conclude that the multiple is 2, i.e., that the Cooper pair is the *only* elementary object in the superconducting state. The presence of higher-order correlations of electrons (four, six, or possibly an odd number) cannot be unambiguously distinguished from the harmonic effects. For example, the tunneling of four correlated electrons and the emission of one photon of frequency ν would occur at voltage $V=h\nu/4e$, while the second harmonic of the Josephson radiation emitted at this voltage would also occur at ν. In the case of radiation-induced steps, the tunneling of four correlated electrons would result in an induced step at exactly the same voltage as the normal subharmonic step of order $\frac{1}{2}$. From the relative amplitude of the observed harmonic and subharmonic effects (e.g., the fact that in tunnel junctions the radiation-induced subharmonic steps are usually absent) it can be concluded that the correlation preferred by several orders of magnitude is the pairing of electrons. Higher-order correlations may exist but their relative importance must be very small. As pointed out in Sec. II A, the experimental results do not exclude the possibility of a nonintegral number of electrons such as $2(1+\epsilon)$, where ϵ is less than 40 ppm. We shall leave further discussions of such exotic possibilities to our theoretically inclined colleagues.

In order to use these measurements as a source of information about the fundamental constants, we must assert that the frequency-voltage ratio is identically equal to $2e/h$. We know of no unassailable way to "prove" this assertion but we believe that the following reasons plus the consistency of the result with all other areas of physics (see II) are convincing evidence. The demonstrated invariance of the frequency-voltage ratio under all experimental conditions strongly suggests that this ratio is equal to a fundamental physical quantity. This physical quantity must be related to the fundamental nature of superconductivity, since it is independent of all material and environmental parameters. Second, all theoretical evidence at present equates the Josephson frequency-voltage ratio exactly to the fundamental constant $2e/h$. In the absence of any theoretical or experimental evidence to the contrary and with the agreement of the experimental result and the accepted value of $2e/h$ to the accuracy with which the latter is confidently known from other experiments, we feel secure in our interpretation of these measurements as a new determination of the fundamental physical constant e/h.

All of the aspects of these measurements combine to form perhaps the most striking demonstration to date of the concept of macroscopic quantum phase coherence in superconductors. The fact that the radiation-induced steps are uniquely defined to better than 1 ppm (for most junctions) and the fractional linewidth of the radiation emitted by the oscillating supercurrent is often less than 1 ppm demands that the relative phase of the two superconductors forming a Josephson junction be an extremely well defined parameter. The generality and invariance of the frequency-voltage ratio dramatically demonstrate that a system of two weakly coupled superconductors is intrinsically a very simple quantum system which is accurately characterized by the relative pair phase. In its essential behavior, a Josephson junction more nearly resembles a simple two-body quantum system than a complex system of 10^{23} strongly interacting particles. Indeed, considered as a two-body system, it is in many respects simpler than the hydrogen atom.

Since the ac Josephson effect does not depend in any essential way on the microscopic properties of a superconductor, but only on the existence of the phase of the macroscopic superconducting wave function, these experiments provide very little additional information about the properties of a superconductor. It is precisely for this reason that the ac Josephson effect can be used to measure a fundamental physical constant.

Note added in proof. Several developments which bear on the subject of this paper have occurred since it was written: (1) F. Bloch [Phys. Rev. Letters **21**,1241 (1968)] has published a simple interpretation of the Josephson effect which may be taken to provide further support for belief in the validity of its theoretical basis. (2) J. Clarke [Phys. Rev. Letters **21**,1566 (1968)] has reported an experiment in which two Josephson junctions composed of different materials (Sn, In, or Pb) were exposed to the same rf field, and the induced steps were compared using a sensitive superconducting galvanometer. The results indicate that the electrochemical potential differences across the two junctions were identical to within one part in 10^8, independent of a variety of experimental parameters. This provides additional support for our conclusions concerning the material and environment independence of our results. (3) M. O. Scully and P. A. Lee (private communication and to be published) have used the quantum theory of the laser to predict that the frequency of a radiating tunnel junction may be pulled slightly from the value 2 eV/h. B. D. Josephson (private communcation) has suggested that the predicted shift may be nearly can-

celled by another contribution. In any case, the fractional size of the shift was estimated at 10^{-9} to 10^{-10}, three to four orders of magnitude below the level with which we have been concerned in our experiments. (4) In its October, 1968 meeting, the Comité International des Poids et Mesures approved a recommendation of the Comité Consultatif d'Electricité of the Bureau International des Poids et Mesures (BIPM) that the BIPM as-maintained volt should be adjusted downwards (effective January 1, 1969) to bring it into better agreement with the absolute volt. The various national standards laboratories are to make simultaneous adjustments of their as-maintained volts for the same reason. The reduction of the NBS as-maintained volt is 8.4 ppm. In terms of the NBS volt as maintained after January 1, 1969, V_{69NBS}, our experimental result becomes $2e/h = 483.5935 \pm 0.0012$ MHz/μV_{69NBS} (2.4 ppm).

ACKNOWLEDGMENTS

We would like to thank Loebe Julie for his cooperation and many helpful discussions concerning the potentiometer, A. G. McNish for arranging the calibration of the standard cells, E. Richard Cohen and Jesse W. M. Dumond for their interest and encouragement, and many of our colleagues at the University of Pennsylvania and elsewhere for stimulating discussions, most especially D. J. Scalapino and J. R. Schrieffer.

PHYSICAL REVIEW VOLUME 177, NUMBER 2 10 JANUARY 1969

Frequency Dependence of the Paramagnetic Relaxation in a Copper Tutton Salt*

THOMAS E. PRATT†
Rutgers University, New Brunswick, New Jersey 08903
(Received 27 November 1967; revised manuscript received 9 September 1968)

Measurements have been made of the paramagnetic relaxation rate of the copper ions in zinc-diluted crystals of copper ammonium sulfate at 1.3°K by a pulsed-microwave technique at frequencies between 9.0 and 11.8 GHz, in order to look for the ν^4 dependence to be expected if the orbit-lattice mechanism and direct process dominate. In the crystals examined, at the highest copper concentration, the rate decreased with increasing frequency. At the lowest concentration, a dependence was obtained which could be fitted with a fourth power, but this behavior was not independent of crystal orientation. A linear temperature dependence of the rate was obtained below 2.1°K.

I. INTRODUCTION

PARAMAGNETIC relaxation in iron-group salts at liquid-helium temperatures has been interpreted usually in terms of the one-phonon, direct process[1] and the orbit-lattice interaction mechanism.[2,3] These predict, respectively, a relaxation rate proportional to the absolute temperature and to the second or fourth power of the external magnetic field or, equivalently, the resonance frequency, depending upon the level structure of the ground state of the ion. The fourth power is appropriate for ions, such as divalent copper, with ground-state doublets split only by a magnetic field. The spin-$\frac{1}{2}$ copper ions in the easily crystallized Tutton salt provide a convenient two-level system for studying relaxation, complicated, however, by cross relaxation[4] arising from the four hyperfine lines and two inequivalent sets of copper ions.

The relaxation rate in the Tutton salt has been studied extensively with respect to dependence upon temperature, crystal size, and copper-ion concentration. Gill[5] has measured the temperature dependence of the rate in macroscopic crystals of the potassium salt for various copper-ion concentrations. The results were a linear behavior at the lowest concentration, 0.01% of possible copper sites occupied, and a higher power law at higher concentrations. Nash[6] measured decay times in crystals of the ammonium salt with variations in copper-ion concentration and crystal size, the latter extending down to tens of microns. A size effect was observed which, at copper-ion concentrations of 5% or less, was significant only in crystals of dimensions of 100 μ or smaller. In these crystals the size effect was suggested to be caused by the presence of impurities.

Calculations of the relaxation rate using the direct process and orbit-lattice mechanism do not yield a size dependence. Consequently, if these are operative, their effects would most likely be seen in crystals of low concentration of the paramagnetic ion and of sufficient size that impurities present no problem.

The purpose of the present experiment was to mea-

* Work supported in part by the U. S. Office of Naval Research under Contract No. Nonr-404(20).
† Present address: Utica College of Syracuse University, Utica, N. Y.
[1] I. Waller, Z. Physik **79**, 370 (1932).
[2] J. H. Van Vleck, Phys. Rev. **58**, 426 (1940).
[3] R. Orbach, Proc. Phys. Soc. (London) **77**, 821 (1961).
[4] N. Bloembergen, S. Shapiro, P. S. Pershan, and J. O. Artman, Phys. Rev. **114**, 445 (1959).
[5] J. C. Gill, Proc. Phys. Soc. (London) **85**, 119 (1965).
[6] F. Nash, Phys. Rev. **138**, A1500 (1965).